Molecular Pharmacology Fast Forward. Published on December 9, 2014 as DOI: 10.1124/mol.114.096784
This article has not been copyedited and formatted. The final version may differ from this version.

Induction of CYP26A1 by Metabolites of Retinoic Acid: Evidence that CYP26A1 is an Important Enzyme in the Elimination of Active Retinoids

Ariel R. Topletz, Sasmita Tripathy, Robert S Foti, Jakob A. Shimshoni, Wendel L. Nelson, and Nina Isoherranen

Departments of Pharmaceutics (ART, ST, JAS, NI) and Medicinal Chemistry (WLN), University of Washington, Seattle, WA; Department of Pharmacokinetics and Drug Metabolism, Amgen Inc, Seattle, WA (RSF)

Molecular Pharmacology Fast Forward. Published on December 9, 2014 as DOI: 10.1124/mol.114.096784
This article has not been copyedited and formatted. The final version may differ from this version.

Running Title Page: Induction of CYP26A1 by *at*RA metabolites

Corresponding Author: Nina Isoherranen, Department of Pharmaceutics, University of Washington, H-272, Box 357610, Seattle, Washington 98195, Phone: 206-543-0829, Fax: 206-543-3204 ni2@u.washington.edu

Text Pages: 27

Figures: 9

References: 42

Abstract Words: 250

Introduction Words: 692

Discussion Words: 1499

Abbreviations:

*at*RA— all-*trans*-retinoic acid

*at*RA-d_5 — deuterated *at*RA (2 and 3 deuteriums at the C-4 and C-18 positions, respectively)

AUC — area under the concentration curve

4-oxo-*at*RA — 4-oxo-all-*trans*-retinoic acid

4-OH-*at*RA — 4-hydroxy-all-*trans*-retinoic acid

(4R)-OH-*at*RA — (4R)-hydroxy-all-*trans*-retinoic acid

(4S)-OH-*at*RA — (4S)-hydroxy-all-*trans*-retinoic acid

18-OH-*at*RA — 18-hydroxy-all-*trans*-retinoic acid

4-oxo-*at*RA-d_3 — deuterated 4-oxo-all-*trans*-retinoic acid (3 deuteriums at the C-18 position)

HepG2 — hepatoblastoma cells

Molecular Pharmacology Fast Forward. Published on December 9, 2014 as DOI: 10.1124/mol.114.096784
This article has not been copyedited and formatted. The final version may differ from this version.

RDH — retinol dehydrogenase

RALDH — retinal dehydrogenase

RAR — retinoic acid receptor

RXR — retinoid “X” receptor

IS — internal standard

LOQ — limit of quantification

LOD — limit of detection

GAPDH — Glyceraldehyde 3-phosphate dehydrogenase

KPi — potassium phosphate

Molecular Pharmacology Fast Forward. Published on December 9, 2014 as DOI: 10.1124/mol.114.096784
This article has not been copyedited and formatted. The final version may differ from this version.

Abstract

all-trans-Retinoic acid (*at*RA), the active metabolite of vitamin A, induces gene transcription via binding to nuclear retinoic acid receptors (RARs). The primary hydroxylated metabolites formed from *at*RA by CYP26A1, and the subsequent metabolite 4-oxo-*at*RA, bind to RARs and potentially have biological activity. Hence CYP26A1, the main *at*RA hydroxylase, may function either to deplete bioactive retinoids or to form active metabolites. The aim of this study was to determine the role of CYP26A1 in modulating RAR activation via formation and elimination of active retinoids. Following treatment of HepG2 cells with *at*RA, (4S)-OH-*at*RA, (4R)-OH-*at*RA, 4-oxo-*at*RA and 18-OH-*at*RA, mRNAs of CYP26A1 and RARβ were increased 300-3000-fold with 4-oxo-*at*RA and *at*RA being the most potent inducers. However, >60% of the 4-OH-*at*RA enantiomers were converted to 4-oxo-*at*RA in the first 12 hours of treatment suggesting that the activity of the 4-OH-*at*RA was due to 4-oxo-*at*RA. In human hepatocytes *at*RA, 4-OH-*at*RA and 4-oxo-*at*RA induced CYP26A1 and 4-oxo-*at*RA formation was observed from 4-OH-*at*RA. In HepG2 cells 4-oxo-*at*RA formation was observed even in the absence of CYP26A1 activity and this formation was not inhibited by ketoconazole. In human liver microsomes 4-oxo-*at*RA formation was supported by NAD^+ suggesting 4-oxo-*at*RA formation is mediated by a microsomal alcohol dehydrogenase. While 4-oxo-*at*RA was not formed by CYP26A1, it was depleted by CYP26A1 (K_m=63 nM and Cl_{int}=90 μL/min/pmol). Similarly, CYP26A1 depleted 18-OH-*at*RA and the 4-OH-*at*RA enantiomers. These data support the role of CYP26A1 to clear bioactive retinoids, and suggest that the enzyme forming active 4-oxo-*at*RA may be important in modulating retinoid action.

Molecular Pharmacology Fast Forward. Published on December 9, 2014 as DOI: 10.1124/mol.114.096784
This article has not been copyedited and formatted. The final version may differ from this version.

Introduction

all-trans-Retinoic acid (*at*RA), the active metabolite of vitamin A (retinol), is an essential signaling molecule during fetal development and adult life. Retinoid signaling plays a role in maintaining healthy skin, epithelia and the immune system (Napoli, 2012), regulating insulin stimulated glucose secretion (Kane et al., 2010), lipid homeostasis (Bonet et al., 2012), embryonic development (Duester, 2008), stem cell and neuronal differentiation (Maden, 2007; Gudas and Wagner, 2011), tissue repair and regeneration (Gudas, 2012) and spermatogenesis (Chung and Wolgemuth, 2004; Hogarth and Griswold, 2013). The biological activity of *at*RA is largely mediated by its binding to the nuclear ligand activated retinoic acid receptors (RARs) and the peroxisome proliferator-activated receptor β/δ (PPAR β/δ) (Schug et al., 2007; Yu et al., 2012). As such retinoid signaling in a specific cell depends on the expression of the nuclear receptors and the concentration of *at*RA within the cell (McBurney, 1993; Rhinn and Dolle, 2012). Hence, it is not surprising that RARs are expressed in a cell-type specific fashion (Chambon, 1996), and *at*RA concentrations vary considerably among retinoid responsive tissues (Kane et al., 2008).

The concentration of *at*RA is regulated by synthesis from retinol via retinaldehyde by alcohol and aldehyde dehydrogenases and elimination by cytochrome P450 (CYP) enzymes (Napoli, 2012). The enzymes of the CYP26 family are primarily responsible for *at*RA clearance forming the hydroxylated metabolites 4-OH-*at*RA, 18-OH-*at*RA, (Figure 1) and perhaps 16-OH-*at*RA (White et al., 1997; White et al., 2000; Chithalen et al., 2002; Thatcher et al., 2011; Topletz et al., 2012). CYP26A1 is the predominant *at*RA hydroxylase in the adult human liver (Thatcher et al., 2010; Topletz et al., 2012), and it is highly inducible by *at*RA via RAR-mediated mechanism (White et al., 1997; Yamamoto et al., 2000; Loudig et al., 2005; Tay et al.,

Molecular Pharmacology Fast Forward. Published on December 9, 2014 as DOI: 10.1124/mol.114.096784
This article has not been copyedited and formatted. The final version may differ from this version.

2010) leading to autoinduction of CYP26A1 by *at*RA. This autoinduction allows for efficient feedback for *at*RA regulating its own clearance but also suggests that *at*RA will induce the formation of potentially active metabolites by CYP26A1. The primary hydroxylation products 4-OH-*at*RA, 18-OH-*at*RA and the sequential metabolite 4-oxo-*at*RA from 4-OH-*at*RA bind to RARs including RARα (Idres et al., 2002). Since CYP26A1 forms metabolites that have RAR binding affinity, it is possible that CYP26A1 may play a role in forming metabolites with specific retinoid activity. However, the biological role of *at*RA metabolites is largely unknown. While genetic studies have shown that the developmental malformations of CYP26A1$^{-/-}$ mice are mainly due to excess *at*RA and not to the lack of formation of an active metabolite (Niederreither et al., 2002), it is not known whether the metabolites are important for specific processes later in life.

Of the metabolites from *at*RA, 4-oxo-*at*RA is the most studied and the most potent in terms of RAR activation, having a three-fold lower EC_{50} than *at*RA towards RARα (Idres et al., 2002). 4-Oxo-*at*RA is also detected in human plasma suggesting it may have biological significance (Muindi et al., 1992b; Arnold et al., 2012). The potential biological importance of 4-oxo-*at*RA is supported by studies that show that 4-oxo-*at*RA is teratogenic in mice and zebrafish with similar potency as *at*RA itself (Creech Kraft et al., 1989; Herrmann, 1995). In human skin cells 4-oxo-*at*RA displays strong transcriptional regulatory activity (Baron et al., 2005) and in *Xenopus* embryos 4-oxo-*at*RA modulates positional specification (Pijnappel et al., 1993). Finally, 4-oxo-*at*RA induces spermatogenesis in vitamin A deficient mice (Gaemers et al., 1996). Whether 4-oxo-*at*RA is formed by CYP26 enzymes is not clear and the processes that regulate the homeostasis of 4-oxo-*at*RA are not well understood. As such the importance of 4-oxo-*at*RA in retinoid biology is poorly defined.

Molecular Pharmacology Fast Forward. Published on December 9, 2014 as DOI: 10.1124/mol.114.096784
This article has not been copyedited and formatted. The final version may differ from this version.

The aim of this study was to determine whether CYP26A1 is induced by oxidated metabolites of *at*RA, and whether CYP26A1 forms and clears the oxidated metabolites including 4-oxo-*at*RA. The results of this study show that oxidated *at*RA metabolites are substrates of CYP26A1, and they induce their own clearance by CYP26A1. However, formation of 4-oxo-*at*RA, the metabolite with high RAR activation potency, is not mediated by CYP26A1 in cells or in the human liver. Taken together these results support the conclusion that CYP26A1 functions primarily to eliminate bioactive retinoids, and that additional enzymes are required to form the bioactive metabolites of *at*RA such as 4-oxo-*at*RA.

Materials and Methods

Chemicals and reagents: *at*RA, ketoconazole, fomepizole (4-methylpyrazole), cimetidine, testosterone, and carbenoxolone were purchased from Sigma-Aldrich (St. Louis, MO). Talarozole was purchased from MedChem Express (Monmouth, NJ). 4-Oxo-*at*RA-d_3 (3 deuteriums at the C-18 position) and *at*RA-d_5 (2 deuteriums at the C-4 and 3 deuteriums at the C-18 positions) were purchased from Toronto Research Chemicals (North York, Ontario). (4R)-OH-*at*RA, (4S)-OH-*at*RA, 4-oxo-*at*RA, and 18-OH-*at*RA (Figure 1) were synthesized as previously described (Shimshoni et al., 2012; Topletz et al., 2012). Optima-grade water, optima-grade acetonitrile, ethanol and ethyl acetate were purchased from Fisher Scientific (Pittsburgh, PA). Biological DNAase/RNAase-free water was purchased from Qiagen (Valencia, CA).

Quantitative analysis of retinoids: *at*RA, 4-oxo-*at*RA, (4R)-OH-*at*RA, (4S)-OH-*at*RA and 18-OH-*at*RA (Figure 1) were extracted from cell and medium samples and from incubations using ethyl acetate under red light as previously described (Thatcher et al., 2010; Topletz et al.,

Molecular Pharmacology Fast Forward. Published on December 9, 2014 as DOI: 10.1124/mol.114.096784
This article has not been copyedited and formatted. The final version may differ from this version.

2012), the solvent was evaporated under nitrogen stream and the dry residue reconstituted in 100 µL of acetonitrile for HPLC-MS/MS analysis.

Analytes were separated using an Agilent 1290 Infinity UHPLC, Agilent Zorbax C18 column (3.5 µm, 2.1 mm x 100 mm) and a mobile phase flow of 0.2 mL/min and a linear 30 min gradient with initial mobile phase of 10:90 acetonitrile:aqueous 0.1% formic acid increasing to 90:10 acetonitrile:aqueous 0.1% formic acid (held for 2 min) followed by a re-equilibration back to initial mobile phase conditions over 3 min. The analytes were detected using an AB Sciex API 5500 Q/LIT mass spectrometer using negative ion electrospray detection, with declustering potentials of -80 V (4-OH-*at*RA and 18-OH-*at*RA), -90 V (4-oxo-*at*RA-d_3), -140 V (*at*RA), -100 V (*at*RA-d_5) and -95 V (4-oxo-*at*RA and 4-oxo-13-*cis*RA); collision energies of -28 eV (4-OH-*at*RA and 18-OH-*at*RA), -25 eV (4-oxo-*at*RA-d_3), -40 eV (*at*RA-d_5) and -22 eV (*at*RA, 4-oxo-*at*RA and 4-oxo-13-*cis*RA); and collision exit potentials of -7 V (*at*RA, 4-OH-*at*RA and 18-OH-*at*RA), -5 V (4-oxo-*at*RA and 4-oxo-13-*cis*RA), -16 V (*at*RA-d_5) and -10 V (4-oxo-*at*RA-d_3). The parent-fragment MS/MS transitions of *m/z* 299 → 255 Da (*at*RA), 304 → 260 Da (*at*RA-d_5), 315 → 253 Da (4-OH-*at*RA and 18-OH-*at*RA), 313 → 269 Da (4-oxo-*at*RA and 4-oxo-13-*cis*RA), and 316 → 272 Da (4-oxo-*at*RA-d_3) were monitored. The lower limits of quantification were 3.1 nM for 4-OH-*at*RA, 0.3 nM for 4-oxo-*at*RA, and 6.3 nM for 18-OH-*at*RA. Standard curves were reproducible within 15% of each other from three separate extractions on three different days of analysis.

Cell culture and mRNA analysis. The HepG2 cells were obtained and cultured in a humidified incubator at 37 °C as previously described (Tay et al., 2010) under an atmosphere of 5% carbon dioxide using ATCC Minimum Essential Medium with Earle's balanced salt solution supplemented with 10% fetal bovine serum and 0.5% penicillin as the growth medium (Tay et

Molecular Pharmacology Fast Forward. Published on December 9, 2014 as DOI: 10.1124/mol.114.096784
This article has not been copyedited and formatted. The final version may differ from this version.

al., 2010). For *at*RA and *at*RA metabolite treatments, cells were plated into six well plates (10^6 cells per well) in 2 mL of medium/well and cells were allowed to adhere for 24 hours prior to treatments. The cells were treated for 48 hours in 2 mL of medium, changing the medium (+ inducer) at 24 hours. The treatments included *at*RA, 4-oxo-*at*RA, (4R)-OH-*at*RA, (4S)-OH-*at*RA, or 18-OH-*at*RA at concentrations of 1 nM to 1 μM or 0.1% EtOH as a vehicle control. All treatments were performed in triplicate. At the completion of each treatment, the medium in each well was aspirated and cells were harvested for mRNA extraction. The time course of CYP26A1 and RARβ induction in HepG2 cells was characterized following a 1 μM treatment with *at*RA. The cells were cultured as above but cells were harvested at 6, 12, 24 and 48 hrs after treatment for mRNA extraction.

Pooled cryopreserved human hepatocytes from two male and one female donor were obtained from Life Technologies (Grand Island, NY). Hepatocytes were thawed at 37°C, placed into plating media (InVitroGro CP medium plus Torpedo antibiotic mix; Bioreclamation IVT, Baltimore, MD) and cell viability confirmed. Hepatocytes were plated at 10^6 live cells per well in 6-well collagen type-I coated plates (Becton Dickinson, Franklin Lakes, NJ) and allowed to attach for ~8 hours. The plating media was then replaced with Williams E media containing cell maintenance supplements (CM4000; LifeTechnologies, Grand Island, NY) and cells treated with *at*RA, 4-OH-*at*RA or 4-oxo-*at*RA each at 100, 500 and 1000 nM or ethanol as a vehicle control for 2 hours. The short, two hour, treatment period was chosen to minimize retinoid depletion and metabolism in the treatments. Immediately after addition of the retinoids and at the end of the 2-hour induction period, an aliquot of the media was collected for retinoid concentration measurements as described above. At the end of the 2-hour induction period the cells were collected for mRNA measurements.

Molecular Pharmacology Fast Forward. Published on December 9, 2014 as DOI: 10.1124/mol.114.096784
This article has not been copyedited and formatted. The final version may differ from this version.

For mRNA extraction, 300 µl of TRI reagent (Invitrogen, Grand Island, NY) was added to each well and mRNA extracted according to the manufacturer's recommendations. Total RNA was quantified using the Nanodrop 2000c Spectrophotometer (Thermofisher Sci., Waltham, MA) and RNA quality was determined by gel electrophoresis. cDNA was generated from 1 µg mRNA using TaqMan® Gene expression reagents (Applied Biosystems, Carlsbad, CA). RT-PCR was used to quantify CYP26A1 and RARβ mRNA (StepOnePlus^{TM}, Applied Biosystems, Carlsbad, CA) as previously described (Tay et al., 2010). TaqMan real-time gene expression master mix and PCR primers and fluorescent probes were obtained from Applied Biosystems (Foster City, CA). Probes were labeled with the 5'-reporter dye 5-carboxyfluorescein and a nonfluorescent black hole quencher on the 3'-end. Primer and probe pairs used included: CYP26A1 (Hs00175627_m1, FAM), GAPDH (Hs99999905_m1, VIC), RARα_ (Hs00940446_m1, FAM), RARβ_ (Hs00233407_m1, FAM), RARγ (Hs00171273_m1, FAM), CRABP-I (Hs00171635_m1, FAM) and CRABP-II (Hs00275636_m1, FAM). GAPDH was used as the housekeeping gene and all assays were done as multiplexes. All triplicate samples were analyzed in duplicate. Changes in target mRNA were measured using relative quantification (fold-difference) and the $\Delta\Delta C_T$ method (Tay et al., 2010) using GraphPad Prism v.5 (La Jolla, CA).

RAR reporter assays. Human RARα, RARβ and RARγ reporter assays (Indigo Biosciences, State College, PA) were used to determine the ability of *at*RA, 4-OH-*at*RA and 4-oxo-*at*RA to act as agonists of human retinoic acid receptors. In brief, reporter cells were rapidly thawed into pre-warmed cell recovery media and plated into a 96-well assay plate (100 µL reporter cell suspension per well). Retinoic acid metabolites (0 – 2 µM, final concentration in compound screening media) were then added to the assay plate. Each reporter assay plate was

Molecular Pharmacology Fast Forward. Published on December 9, 2014 as DOI: 10.1124/mol.114.096784
This article has not been copyedited and formatted. The final version may differ from this version.

placed in a humidified incubator (37 ºC / 5% CO_2) for approximately 20 hours. Assay plates were then removed from the incubator and the contents aspirated from each well. Luciferase detection reagent (100 µL) was added to each well and the plates allowed to rest at room temperature for 30 minutes. Luminescence was then measured on a Tecan Safire2 plate reader (Tecan, San Jose, CA) set to quantify luminescence using a read time of 500 msec per well.

Retinoid depletion and subsequent metabolite formation in HepG2 cells. Depletion of *at*RA, 4-oxo-*at*RA, (4R)-OH-*at*RA, (4S)-OH-*at*RA, or 18-OH-*at*RA and formation of subsequent metabolites from these substrates in HepG2 cells was measured in the media and in the cells to assess the exposure of the cells to the bioactive retinoids. HepG2 cells were plated and cultured as described above. Cells were treated with *at*RA, 4-oxo-*at*RA, (4R)-OH-*at*RA, (4S)-OH-*at*RA, or 18-OH-*at*RA at a concentration of 1 µM (nominal initial concentration in the medium) for 48 hours. The medium (+ inducer) was changed after 24 hours to mimic the design of the mRNA induction experiments. At 0, 1, 4, 8, 12, 24, and 48 hours, 1 mL of the medium was removed, an internal standard (*at*RA-d_5; 20 µL of a 2.5 µM stock solution) was added, and samples were extracted using ethyl acetate as described above. As controls, 4-oxo-*at*RA, (4R)-OH-*at*RA or (4S)-OH-*at*RA (1 µM) were incubated in 1 mL of medium each for four hours in a 37 ºC oscillating water bath and the media were analyzed for substrate depletion and metabolite formation. Cells were collected at 1, 4, 8, and 12 hours after the beginning of the treatments by addition of 1 mL of acetonitrile on the cells in each well. One milliliter of KPi buffer (100 mM, pH 7.4) was added to the acetonitrile phase to facilitate separation of the organic and aqueous layers, an internal standard (4-oxo-RA-d_3; 20 µL of a 2.5 µM stock solution) was added, and samples were extracted with ethyl acetate as described previously. The amounts of analytes in

Molecular Pharmacology Fast Forward. Published on December 9, 2014 as DOI: 10.1124/mol.114.096784
This article has not been copyedited and formatted. The final version may differ from this version.

the extract were determined by LC-MS/MS and the retinoid concentrations in the cells were calculated using a total intercellular volume of 1 µL/10^6 HepG2 cells (Kewn et al., 2000).

Measurement of CYP26A1 activity in HepG2 cells. The formation of 4-OH-*at*RA-d_4 and 4-oxo-*at*RA-d_3 from *at*RA-d_5 was used to determine CYP26A1 activity and induction during treatment of HepG2 cells with *at*RA. HepG2 cells were treated for 48 hours with *at*RA (1 µM final concentration in the medium). The medium containing *at*RA was changed at 24 hours. At 0.5, 6, 12, 18, 24, 36, and 48 hours, *at*RA-d_5 (100 nM) was added to each well (3 mL) and formation of 4-OH-*at*RA-d_4 and 4-oxo-*at*RA-d_3 after a 1 hour incubation was measured. All incubations were conducted in triplicate. An initial aliquot of the medium (1 mL) was removed 30 seconds after *at*RA-d_5 addition as a control, and after one hour at 37 ºC, a second aliquot of medium (1 mL) was removed from each well. 4-Oxo-13-*cis*RA (20 µL of a 2.5 µM stock solution in EtOH) was added to each sample as an internal standard, and samples were extracted using 3 mL of ethyl acetate and analyzed using HPLC-MS/MS as described above. 4-Oxo-*at*RA-d_3 was quantified using a reference material. Due to the lack of a standard, the relative change in formation of 4-OH-*at*RA-d_4 was determined from the analyte to internal standard peak height ratio. Standard curves were constructed for *at*RA-d_5 and 4-oxo-*at*RA-d_3. The rate of 4-oxo-*at*RA-d_3 formation from 4-OH-*at*RA-d_4 was assumed to remain constant during treatment.

Characterization of 4-oxo-*at*RA formation from 4-OH-*at*RA in HepG2 cells. To determine whether formation of 4-oxo-*at*RA is predominantly P450-mediated in HepG2 cells, the HepG2 cells were incubated with *at*RA or 4-OH-*at*RA (1 µM in the medium with 0.1% EtOH) for 24 hours in the presence and absence of ketoconazole (10 µM in the medium with 0.1% EtOH), a potent pan-P450 inhibitor (Thatcher et al., 2011). In addition, HepG2 cells were incubated in the presence of *at*RA and 4-OH-*at*RA with vehicle or alcohol dehydrogenase

Molecular Pharmacology Fast Forward. Published on December 9, 2014 as DOI: 10.1124/mol.114.096784
This article has not been copyedited and formatted. The final version may differ from this version.

inhibitors 4-methylpyrazole (250 μM) and cimetidine (250 μM), the aldo-keto-reductase inhibitor testosterone (25 μM), and the retinol dehydrogenase inhibitor carbenoxolone (25 and 50 μM) and in the presence of *at*RA with talarozole (1 μM) a selective CYP26 inhibitor. All treatments were performed in triplicate. An initial aliquot of the medium (0.5 mL) was taken before medium was added to each well to quantify the initial substrate concentrations per well. After 24 hours, a second aliquot of the medium (0.5 mL) was removed and extracted with ethyl acetate. Standard curves were constructed for *at*RA, 4-oxo-*at*RA and 4-OH-*at*RA with an internal standard of 4-oxo-*at*RA-d_3 (20 μL of a 2.5 μM stock solution). All samples were separated and analyzed for 4-OH-*at*RA and 4-oxo-*at*RA formation using the HPLC-MS/MS method described above.

Characterization of 4-oxo-RA and 18-OH-RA as CYP26A1 substrates.

The metabolism of 4-oxo-*at*RA and 18-OH-*at*RA by CYP26A1 was evaluated by substrate depletion using a similar protocol as previously described for characterization of 4-OH-*at*RA depletion (Shimshoni et al., 2012; Topletz et al., 2012). The Bac-to-Bac Baculovirus Expression System (Invitrogen) with Sf9 insect cells was used to produce His-tagged CYP26A1 protein according to the manufacturer's instructions using Sf-900 II SFM liquid media (Invitrogen) supplemented with 2.5% fetal bovine serum. During protein expression, ferric citrate (0.2 mM) and δ-aminolevulinic acid (0.3 mM) were added to the media 24 hours post-infection to facilitate heme synthesis. The cells were harvested 72 hours post infection, washed once in PBS with 1 mM phenylmethanesulphonylfluoride, pelleted and stored at –80°C. Insect cell microsomes were prepared by standard ultracentrifugation at 120,000g and supplemented with P450 reductase prior to incubations. The P450 content of the final microsomal preparation was determined by CO-difference spectrum.

Molecular Pharmacology Fast Forward. Published on December 9, 2014 as DOI: 10.1124/mol.114.096784
This article has not been copyedited and formatted. The final version may differ from this version.

For quantification of the substrates, standard curves for each substrate were prepared in 100 mM KPi buffer (pH 7.4) containing CYP26A1 (2 pmol/mL enzyme and 4 pmol/mL rat reductase) as previously described (Lutz et al., 2009; Thatcher et al., 2011). In brief, incubations containing substrate, 2 pmol/mL CYP26A1 in the endoplasmic reticulum membrane and 4 pmol/mL of purified rat reductase in 100 mM KPi buffer (pH 7.4) were pre-incubated for 5 min at 37ºC before the addition of NADPH (final concentration of 1 mM) to initiate the reaction. Each sample initially contained a total volume of 2 mL, and 4-oxo-*at*RA and 18-OH-*at*RA were added at concentrations ranging from 5 to 150 nM. At 0.5, 1, 2, and 5 min, aliquots of 0.5 mL were collected and immediately quenched in a test tube containing 3 mL of ice-cold ethyl acetate. For the final time point, ethyl acetate was added directly to the incubation vial. The internal standard 4-oxo-*at*RA-d_3 (20 µL of a 2.5 µM stock solution in EtOH) was added, and samples were extracted as described above. All incubations were conducted in duplicate and 4-oxo-*at*RA and 18-OH-*at*RA were quantified using standard curves.

Retinoids from the in vitro incubations were analyzed using LC-MS/MS as described above for cell culture experiments except that analytes were detected using positive ion electrospray mass spectrometry, with the declustering potentials of 80 V, collision energies of 20 eV (18-OH-*at*RA), 35 eV (4-oxo-*at*RA-d_3) and 37 eV (4-oxo-*at*RA); collision exit potentials of 13 V (18-OH-RA and 4-oxo-*at*RA) and 2 (4-oxo-*at*RA-d_3). The parent-fragment MS/MS transitions of *m/z* 317 → 253 Da (18-OH-*at*RA), 315 → 121 Da (4-oxo-*at*RA) and 300 → 226 Da (4-oxo-*at*RA-d_3) were monitored.

Formation of 4-oxo-*at*RA from 4-OH-*at*RA in human liver microsomes. Human liver microsomes (0.2 mg/mL) were incubated with 4-OH-*at*RA (500 nM) and NADPH, $NADP^+$ or NAD^+ (each at 2 mM) in 100 mM KPi buffer pH 7.4. In addition, 4-OH-*at*RA was incubated

Molecular Pharmacology Fast Forward. Published on December 9, 2014 as DOI: 10.1124/mol.114.096784
This article has not been copyedited and formatted. The final version may differ from this version.

with human liver microsomes in the presence and absence of talarozole (1 μM), a CYP26A1 specific inhibitor, and ketoconazole (10 μM) a pan-P450 inhibitor and with NADPH as a cofactor. Following a 5 min preincubation, the reactions were initiated with the addition of cofactor and incubated for 30 minutes. At 30 min the reactions were quenched with equal volume of acetonitrile and centrifuged at 3,000 g for 15 min. The supernatants were collected and 4-oxo-*at*RA formation was analyzed by LC-MS/MS as described above. All incubations were normalized to a no cofactor control.

Data analysis. Mass spectrometry data was analyzed using Analyst software. Peak heights were used to determine the ratio of substrate to the internal standard. The areas under the medium and cell concentration versus time curves from 0-12 hrs ($AUC^{0\text{-}12hr}$) of *at*RA, (4R)-OH-*at*RA, (4S)-OH-*at*RA, 4-oxo-*at*RA, and 18-OH-*at*RA were calculated by non-compartmental analysis using Phoenix/WinNonLin 6.3 (Pharsight, Mountain View, CA). The cell to medium ratio was calculated for each inducer and for their subsequent metabolites using their respective $AUCs^{0\text{-}12hr}$ in HepG2 cells and the media. One-way analyses of variance coupled with Bonferroni's Multiple Comparison Test were conducted using GraphPad Prism v.5 (La Jolla, CA) to determine significant differences in mRNA expression. Significant changes in 4-oxo-*at*RA formation from *at*RA or 4-OH-*at*RA in the presence of inhibitors compared to no inhibitor controls were compared using Student's unpaired t-test. A p-value of <0.05 was considered significant. The K_m values for 4-oxo-*at*RA and 18-OH-*at*RA were determined from the depletion data as previously described (Shimshoni et al., 2012).

Molecular Pharmacology Fast Forward. Published on December 9, 2014 as DOI: 10.1124/mol.114.096784
This article has not been copyedited and formatted. The final version may differ from this version.

Results

Induction of CYP26A1 and RARβ in HepG2 cells and human hepatocytes and RAR activation by *at*RA and its metabolites. The mRNA of CYP26A1 and RARβ was significantly ($p < 0.05$) increased after 48 hour treatment of HepG2 cells with *at*RA, 4-oxo-*at*RA, (4R)-OH-*at*RA, (4S)-OH-*at*RA, and 18-OH-*at*RA (1 μM), with *at*RA resulting in the greatest induction (Figure 2). The induction of CYP26A1 and RARβ was retinoid concentration dependent (Figures 2B and 2C). The magnitude of CYP26A1 induction following 4-oxo-*at*RA treatment (2980-fold, 1 μM treatment) was ~80 % of that following *at*RA treatment (3700-fold, 1 μM treatment), whereas the induction of CYP26A1 after 4-OH-*at*RA (both enantiomers) and 18-OH-*at*RA treatment was much less, 9-36% of that observed following *at*RA treatment (Figure 2A). The magnitude of induction of CYP26A1 mRNA between (4R)-OH-*at*RA and (4S)-OH-*at*RA treatments was similar ($p > 0.05$). *at*RA and its metabolites also induced RARβ mRNA in a concentration-dependent manner, but the magnitude of RARβ induction was much less, about 3-18% of that observed with CYP26A1 (Figure 2). There were no significant changes in RARα or RARγ mRNA upon treatment with *at*RA or any of the *at*RA metabolites (data not shown).

Similar to HepG2 cells *at*RA, 4-oxo-*at*RA and 4-OH-*at*RA significantly increased CYP26A1 and RARβ mRNA in human hepatocytes (Figure 3) and the magnitude of CYP26A1 induction was approximately 5-fold greater than RARβ induction. In human hepatocytes there was no significant induction of CRABP-I or CRABP-II by any of the three compounds. Following the 2 hr treatment of human hepatocytes *at*RA resulted in the greatest induction of CYP26A1 (16-fold, 1 μM treatment) while 4-OH-*at*RA was a weaker inducer (12-fold induction). The magnitude of CYP26A1 induction was substantially less in human hepatocytes after 2 hr treatment than in HepG2 cells after a 48 hr treatment.

Molecular Pharmacology Fast Forward. Published on December 9, 2014 as DOI: 10.1124/mol.114.096784
This article has not been copyedited and formatted. The final version may differ from this version.

In reporter cell lines *at*RA was the most potent activator of all three RARs. 4-Oxo-*at*RA was 3-8 fold less potent than *at*RA (Figure 4 and Table 1). 4-OH-*at*RA was the least potent activator of all three RARs. It was 2-6 fold less potent than 4-oxo-*at*RA and 6-50 fold less potent than *at*RA in activating the three RARs (Table 1).

Retinoid concentrations and exposure in HepG2 cells and hepatocytes. To determine whether the specific metabolites used in the HepG2 cell treatments were responsible for CYP26A1 and RARβ induction, retinoid concentrations and $AUC^{0\text{-}12hr}$ both in the medium and in cells were quantified following treatment with *at*RA or the metabolites (Table 2, Figure 5). The initial concentration of each treatment was 1 μM, but due to significant depletion of the inducers during incubations the average concentration in cells during treatment was within physiological concentrations of these compounds. In terms of absolute concentrations, *at*RA had the highest cell $AUC^{0\text{-}12hr}$ (3750 ± 350 nmoles•hour/mL) whereas (4S)-OH-*at*RA had the lowest $AUC^{0\text{-}12hr}$ (300 ± 10 nmoles•hour/mL) (Table 2). Although exposures to the 4-OH-*at*RA enantiomers were 90% lower than to *at*RA, the magnitude of CYP26A1 induction following treatment with 4-OH-*at*RA enantiomers was nearly 40% of that observed following *at*RA treatment, suggesting that 4-OH-*at*RA enantiomers or their metabolites are more potent activators of RAR than *at*RA. The cell $AUC^{0\text{-}12hr}$ of 4-oxo-*at*RA (980 ± 40 nmoles•hour/mL) was 60% lower than that of *at*RA, but treatment with 4-oxo-*at*RA resulted in a similar induction of CYP26A1 and RARβ as *at*RA, suggesting that 4-oxo-*at*RA is a more potent inducer of CYP26A1 and RARβ than *at*RA (Table 2). The cell-to-medium concentration ratio ranged from 70 for (4S)-OH-*at*RA to 360 for *at*RA demonstrating differential partitioning of these retinoids into cells (Table 2).

Molecular Pharmacology Fast Forward. Published on December 9, 2014 as DOI: 10.1124/mol.114.096784
This article has not been copyedited and formatted. The final version may differ from this version.

Depletion of *at*RA was not observed during the first 12 hours of treatment (Figures 5 and 6) and no formation of 4-OH-*at*RA or 4-oxo-*at*RA was detected in the medium during this time. In the cells 4-OH-*at*RA and 4-oxo-*at*RA were detected at concentrations of about 3% of *at*RA following 12 hours of *at*RA treatment suggesting minimal CYP26 activity at baseline in the HepG2 cells. Similar to *at*RA depletion, minimal depletion (up to 30 %) of 4-oxo-*at*RA and 18-OH-*at*RA was observed in medium and cells during the first 12 hours of treatment (Figures 5 and 6). Depletion of the 4-OH-*at*RA enantiomers was much more rapid than observed for *at*RA, 4-oxo-*at*RA or 18-OH-*at*RA. During the first 12 hours of treatment 86% of (4S)-OH-*at*RA and 65% of (4R)-OH-*at*RA were depleted (Figures 5 and 6). This depletion was accompanied by increased 4-oxo-*at*RA concentrations in the cells and medium, and the concentrations of 4-oxo-*at*RA in the cells were similar to those of 4-OH-*at*RA following treatments with the 4-OH-*at*RA enantiomers (Figure 5).

After the first 24 hours of treatment, increased depletion of *at*RA (61%) was detected (Figure 6) and 4-OH-*at*RA, 4-oxo-*at*RA and 18-OH-*at*RA were detected as metabolites of *at*RA both in cells and the medium. The depletion of 18-OH-*at*RA and 4-oxo-*at*RA was increased after 24 and 48 hours of treatment; 62% of 18-OH-*at*RA and 29% of 4-oxo-*at*RA was depleted at 24 hours and over 94% of both compounds were depleted at 48 hours (Figure 6). (4R)-OH-*at*RA depletion was 89 % and (4S)-OH-*at*RA 87 % after 24 hours of treatment (Figure 6).

In human hepatocytes depletion of *at*RA, 4-OH-*at*RA and 4-oxo-*at*RA, and formation of metabolites was observed already at 2 hours of treatment (Table 3). The medium exposure ($AUC^{0\text{-}2hrs}$) for 4-oxo-*at*RA was approximately 50% lower than that of *at*RA at all treatment concentrations while the exposure to 4-OH-*at*RA was similar to that of *at*RA.

Molecular Pharmacology Fast Forward. Published on December 9, 2014 as DOI: 10.1124/mol.114.096784
This article has not been copyedited and formatted. The final version may differ from this version.

Time course of CYP26A1 and RARβ induction in HepG2 cells. To determine whether the time course of depletion for *at*RA, 4-oxo-*at*RA and 18-OH-*at*RA could be explained by induction of CYP26A1 activity, the time course of CYP26A1 activity and CYP26A1 and RARβ mRNA was quantified. The time course of CYP26A1 mRNA induction in HepG2 cells is shown in Figure 7 together with the time course of RARβ and CRABP-II induction. CYP26A1 activity was measured by quantifying the formation of 4-oxo-*at*RA-d_3 and 4-OH-*at*RA-d_4 from *at*RA-d_5 at designated time points over a 48 hour treatment with *at*RA (1 μM). Formation of 4-OH-*at*RA-d_4 was slow but detectable during the first 12 hours after initial treatment with *at*RA. It then increased approximately 7-fold ($p < 0.05$) at 24 hours and 33-fold ($p < 0.05$) at 48 hours after the initial treatment with *at*RA (Figure 7). Formation of 4-oxo-*at*RA-d_3 increased similarly as 4-OH-*at*RA-d_4, approximately 7-fold ($p < 0.05$) at 24 hours and 22-fold ($p < 0.05$) at 48 hours after the treatment with *at*RA (Figure 7C). The ratio of 4-OH-*at*RA-d_4 to 4-oxo-*at*RA-d_3 did not change with time. The time course of CYP26A1 activity was in agreement with *at*RA and 18-OH-*at*RA depletion but not with 4-OH-*at*RA depletion.

Formation of 4-oxo-*at*RA from 4-OH-*at*RA in HepG2 cells, human hepatocytes and human liver microsomes. The major metabolite formed from both 4-OH-*at*RA enantiomers was 4-oxo-*at*RA and the metabolism of 4-OH-*at*RA enantiomers was stereoselective. The cell and medium AUCs for (4S)-OH-*at*RA were lower than those for (4R)-OH-*at*RA suggesting a greater clearance of (4S)-OH-*at*RA in HepG2ccells. The $AUC^{0\text{-}12hr}$ of 4-oxo-*at*RA as a metabolite of (4S)-OH-*at*RA was 2.1-fold higher than (4S)-OH-*at*RA cell $AUC^{0\text{-}12hr}$ (Table 2, metabolite to parent ratio 2.1), while the $AUC^{0\text{-}12hr}$ of 4-oxo-*at*RA was 40 % lower than (4R)-OH-*at*RA in cells treated with (4R)-OH-RA (Table 2, metabolite to parent ratio 0.6). Consistent with the HepG2 cell metabolite-to-parent ratios, in the medium 4-oxo-*at*RA $AUC^{0\text{-}12hr}$ was 25% lower

Molecular Pharmacology Fast Forward. Published on December 9, 2014 as DOI: 10.1124/mol.114.096784
This article has not been copyedited and formatted. The final version may differ from this version.

than (4R)-OH-*at*RA $AUC^{0\text{-}12hr}$ while 4-oxo-*at*RA and (4S)-OH-*at*RA had equal AUCs. Based on these data, following (4S)-OH-*at*RA treatment, 4-oxo-*at*RA is the predominant retinoid in the cells, and the formation clearance of 4-oxo-*at*RA from (4S)-OH-*at*RA is higher than the formation clearance of 4-oxo-*at*RA from (4R)-OH-*at*RA. Interestingly, 4-OH-*at*RA was also detected as a reductive metabolite in HepG2 cells treated with 4-oxo-*at*RA and had an $AUC^{0\text{-}12hr}$ that was 40% of that of 4-oxo-*at*RA in cells (Table 2, Figure 4). No degradation of 4-oxo-*at*RA, (4R)-OH-*at*RA, or (4S)-OH-*at*RA was observed in the medium in the absence of cells (data not shown), indicating that the reversible oxidation/reduction seen in HepG2 cells is cell-mediated.

In human hepatocytes treated with *at*RA for 2 hours only 4-oxo-*at*RA was detected as a metabolite, while in 4-OH-*at*RA treated hepatocytes significant formation of 4-oxo-*at*RA was observed at 2 hours of treatment. 4-oxo-*at*RA concentrations in the media were 5-10% of those of 4-OH-*at*RA following 4-OH-*at*RA treatment (Table 3). Formation of 4-OH-*at*RA was also observed in the 4-oxo-*at*RA treated cells (Table 3).

To determine whether formation of 4-oxo-*at*RA from 4-OH-*at*RA enantiomers is P450 mediated, HepG2 cells were first co-incubated with ketoconazole and *at*RA or racemic 4-OH-*at*RA. As formation of 4-OH-RA from *at*RA is predominantly CYP26A1-mediated, inhibition of 4-OH-*at*RA formation from *at*RA by ketoconazole was used as a positive control for CYP26A1 inhibition. In cells treated with *at*RA, ketoconazole decreased 4-OH-*at*RA formation by 84% ($p < 0.05$) and subsequent 4-oxo-*at*RA formation by 80 % ($p < 0.05$) in comparison to the control cells (Table 4). Yet ketoconazole had no effect on 4-oxo-*at*RA formation in cells treated with 4-OH-*at*RA. The depletion of 4-OH-*at*RA was decreased by 25% ($p < 0.05$) by ketoconazole in agreement with a fraction of 4-OH-*at*RA cleared by CYP26A1 to products other than 4-oxo-*at*RA. When HepG2 cells were cotreated with *at*RA and talarozole, a CYP26 specific

Molecular Pharmacology Fast Forward. Published on December 9, 2014 as DOI: 10.1124/mol.114.096784
This article has not been copyedited and formatted. The final version may differ from this version.

inhibitor, 4-OH-RA and 4-oxo-RA formation was significantly decreased confirming that 4-OH-*at*RA formation in these cells is predominantly CYP26A1 mediated (Table 4). None of the other inhibitors tested decreased 4-oxo-*at*RA formation from 4-OH-*at*RA or *at*RA (Table 4).

To further evaluate the enzymes responsible for 4-oxo-*at*RA formation from 4-OH-*at*RA in the human liver, human liver microsomes were incubated with 4-OH-*at*RA in the presence of three different cofactors, NADPH, $NADP^+$ and NAD^+. All three cofactors supported 4-oxo-*at*RA formation (Figure 8) but formation of 4-oxo-*at*RA in the presence of NAD^+ was up to 4-fold higher than in the presence of NADPH or $NADP^+$. Talarozole, a preferential CYP26A1 inhibitor did not inhibit the NADPH mediated formation of 4-oxo-*at*RA from 4-OH-*at*RA while ketoconazole, a pan-P450 inhibitor, decreased the NADPH mediated formation of 4-oxo-*at*RA by 50%.

Metabolism of 4-oxo-*at*RA and 18-OH-*at*RA by CYP26A1. The depletion of 4-oxo-*at*RA and 18-OH-*at*RA in HepG2 cells was observed following increased CYP26A1 activity, suggesting that both 18-OH-*at*RA and 4-oxo-*at*RA were cleared by CYP26A1. To determine the role of CYP26A1 in clearing 18-OH-*at*RA and 4-oxo-*at*RA, the depletion kinetics of both compounds was determined using recombinant CYP26A1 (Figure 9). Both 18-OH-*at*RA and 4-oxo-*at*RA were efficiently depleted by CYP26A1. The K_m values for 4-oxo-*at*RA and 18-OH-*at*RA depletion by CYP26A1 were 63.0 nM and 38.5 nM, respectively. Intrinsic clearance by CYP26A1 was 2.5-fold higher for 18-OH-*at*RA (230 ± 43 µL/min/pmol P450) than for 4-oxo-*at*RA (90 ± 9.0 µL/min/pmol P450).

Molecular Pharmacology Fast Forward. Published on December 9, 2014 as DOI: 10.1124/mol.114.096784
This article has not been copyedited and formatted. The final version may differ from this version.

Discussion

This study shows that metabolites of *at*RA induce RARβ and CYP26A1 mRNA but only 4-oxo-*at*RA is an equipotent or more potent inducer than *at*RA. The induction of CYP26A1 mRNA observed in the HepG2 cells after *at*RA treatment is consistent with previous studies of CYP26A1 induction by *at*RA (Tay et al., 2010; Zhang et al., 2010). Similarly, the lower magnitude of RARβ induction when compared to CYP26A1 is in agreement with previous results (Chambon, 1996; Tay et al., 2010). The fold-induction of CYP26A1 was higher in HepG2 cells than in human hepatocytes but overall the results in human hepatocytes supported the findings in HepG2 cells. The lower fold-induction in hepatocytes may be due to higher baseline expression of CYP26A1 in hepatocytes when compared to HepG2 cells or the much shorter induction time (2hrs) in hepatocytes than in HepG2 cells (48hrs). As shown in Figure 6 the mRNA induction peaks at 48 hours in HepG2 cells. However the short incubation time was chosen for hepatocytes to minimize metabolism and depletion of the inducers.

Induction of CYP26A1 and RARβ mRNA in HepG2 cells has previously been shown to be RARα-mediated (Tay et al., 2010) and the potency of CYP26A1 induction by the metabolites of *at*RA is expected to follow the binding affinity of the metabolites to RARα. Based on previous studies in transfected COS-7 cells, which are expected to have minimal CYP26A1 activity, 4-oxo-*at*RA is the most potent activator of RARα (EC_{50} =33 nM), with *at*RA and 18-OH-RA being 5-fold less potent (EC_{50}=169nM and 162nM, respectively) (Idres et al., 2002). However, in the current study in the reporter assays, *at*RA was about 3-fold more potent RARα agonist and 8-fold more potent RARβ agonist than was 4-oxo-*at*RA. Yet, in human hepatocytes *at*RA and 4-oxo-*at*RA had similar potency as CYP26 inducers. In HepG2 cells 18-OH-*at*RA was significantly less potent than *at*RA or 4-oxo-*at*RA in inducing CYP26A1 and RARβ, while 4-

Molecular Pharmacology Fast Forward. Published on December 9, 2014 as DOI: 10.1124/mol.114.096784
This article has not been copyedited and formatted. The final version may differ from this version.

oxo-*at*RA and *at*RA were equipotent. These differences between studies and cell lines could be due to differential partitioning of the compounds into cells or expression of cellular retinoic acid binding proteins (CRABPs). CRABPs may affect RAR activation and bind *at*RA with higher affinity than the metabolites. However, no CRABP-II induction was observed in HepG2 cells and CRABP-I was not expressed in HepG2 cells suggesting changes in binding protein expression do not contribute to observed induction.

In transfected COS-7 cells 4-OH-*at*RA was the least potent activator of RARα (EC_{50}=791nM) (Idres et al., 2002). Similarly in our studies 4-OH-*at*RA was the least potent RAR agonist for all three RAR isoforms. However, in our studies in HepG2 cells the CYP26A1 induction following 4-OH-*at*RA treatment was approximately one-third of that observed with *at*RA, and in human hepatocytes the induction of CYP26A1 by 4-OH-*at*RA was about 30% less than that observed after 1μM *at*RA treatment. This difference between the reporter cell systems and HepG2 cells or hepatocytes is likely due to differences in formation of 4-oxo-*at*RA, as all the data presented here support the interpretation that induction of RAR target genes after 4-OH-*at*RA treatments is largely due to the formation of 4-oxo-*at*RA.

Previous studies have shown that *at*RA, 4-OH-*at*RA, 18-OH-*at*RA and 4-oxo-*at*RA are substrates of CYP26A1, and CYP26A1 forms a variety of diols and oxo-alcohols from these metabolites (Lutz et al., 2009; Shimshoni et al., 2012; Topletz et al., 2012). While synthetic standards are not available for these sequential metabolites, the depletion clearance of the metabolites can be used to evaluate the role of CYP26A1 in their clearance. Using recombinant CYP26A1, *at*RA and (4S)-OH-*at*RA were found to have the highest CL_{int} (1.2-1.4mL/min/pmol) and 4-oxo-*at*RA the lowest CL_{int} (0.09mL/min/pmol) by CYP26A1. Interestingly, in HepG2 cells 4-OH-*at*RA had more than 2-fold higher clearance than *at*RA, and the CL of *at*RA was of

Molecular Pharmacology Fast Forward. Published on December 9, 2014 as DOI: 10.1124/mol.114.096784
This article has not been copyedited and formatted. The final version may differ from this version.

similar magnitude as 4-oxo-*at*RA. The high clearance of 4-OH-*at*RA and 4-oxo-*at*RA in comparison to *at*RA in HepG2 cells suggests that multiple enzymes are involved in their elimination, and that the induction state of CYP26A1 affects the relative importance of CYP26A1 in retinoid clearance. It is well established that CYP26A1 is the main enzyme that clears *at*RA, and ketoconazole and talarozole effectively inhibited the metabolism of *at*RA in HepG2 cells confirming the role of CYP26A1. Incubations with labeled *at*RA showed that there is minimal baseline CYP26A1 activity in HepG2 cells, a finding in agreement with the induction time-course of CYP26A1 mRNA. In contrast, based on the data presented, there are additional enzymes already at baseline in the cells that clear 4-oxo-*at*RA and 4-OH-*at*RA. It is possible that glucuronidation of 4-OH-*at*RA (and the other retinoids via acyl glucuronides) contributes to 4-OH-*at*RA clearance in HepG2 cells and in hepatocytes, as UGT2B7 has been shown to glucuronidate 4-OH-*at*RA (Samokyszyn et al., 2000) and glucuronides are common in vivo metabolites of *at*RA. In addition, other additional enzymatic processes in the clearance of 4-OH-*at*RA and 4-oxo-*at*RA are supported by the observation of the reduction of 4-oxo-*at*RA back to 4-OH-*at*RA in the treated HepG2 cells and human hepatocytes, a reaction that is not likely to be P450 mediated. However, CYP26A1 appears to contribute to the clearance of 4-oxo-*at*RA and 4-OH-*at*RA as the CL of these compounds was significantly greater after 48 hours of *at*RA treatment than during the first 24 hours.

Despite the fact that all metabolites are substrates of CYP26A1 and their clearances increase with increasing CYP26A1 activity, formation of 4-oxo-*at*RA from 4-OH-*at*RA appears not to be CYP26A1 mediated in HepG2 cells or in human liver. In HepG2 cells there was no change in 4-oxo-*at*RA formation from 4-OH-*at*RA in the presence of the CYP-inhibitor ketoconazole. Surprisingly, the formation of 4-oxo-*at*RA from 4-OH-*at*RA was also not

Molecular Pharmacology Fast Forward. Published on December 9, 2014 as DOI: 10.1124/mol.114.096784
This article has not been copyedited and formatted. The final version may differ from this version.

decreased in the presence of inhibitors of several alcohol dehydrogenases, aldo-ketoreductases, or membrane-bound retinol dehydrogenases in HepG2 cells, suggesting that the enzyme responsible for 4-oxo-*at*RA formation is yet to be identified. In human liver microsomes the formation of 4-oxo-*at*RA was supported by NAD^+ and to a lesser extent $NADP^+$ and NADPH suggesting that a microsomal alcohol dehydrogenase may be responsible for majority of 4-oxo-*at*RA formation in human liver. These findings are in agreement with a previous report in which 4-oxo-*at*RA formation was found to be NAD^+ and $NADP^+$ mediated in hamster liver microsomes (Roberts et al., 1980). However, in contrast to the hamster liver microsomes, in human liver there are also P450 enzymes that can carry out this reaction as shown by the fact that NADPH could support the 4-oxo-*at*RA formation and this formation was inhibited partially by ketoconazole. Yet, no inhibition of 4-oxo-*at*RA formation was observed with talarozole, a CYP26A1 inhibitor showing that the formation of 4-oxo-*at*RA is not mediated by CYP26A1.

The formation of 4-oxo-*at*RA by a novel enzyme is noteworthy as 4-oxo-*at*RA is the only non-glucuronidated *at*RA metabolite detected in human plasma (Muindi et al., 1992a; Muindi et al., 2008; Arnold et al., 2012). 4-Oxo-*at*RA accounts for 10-20% of the *at*RA dose in vivo, both in plasma and as 4-oxo-RA-glucuronide in the urine (Muindi et al., 1992a; Muindi et al., 2008; Arnold et al., 2012), making it a significant metabolite. The abundance of 4-oxo-*at*RA together with its proven biological activity in animal models suggests that 4-oxo-*at*RA formation may contribute to some of the observed retinoid effects in vivo. The conclusive determination of the biological importance of 4-oxo-*at*RA in vitamin A activity will require identification of the specific enzyme(s) that form this metabolite from 4-OH-*at*RA.

The findings presented showing that *at*RA and its metabolites induce CYP26A1 expression and hence their own clearance has implications in the broader context of

Molecular Pharmacology Fast Forward. Published on December 9, 2014 as DOI: 10.1124/mol.114.096784
This article has not been copyedited and formatted. The final version may differ from this version.

understanding *at*RA resistance during therapy with *at*RA. The autoinduction of *at*RA clearance limits efficacy of *at*RA in various cancer treatments. The data presented here suggests that induction of CYP26A1 that results in increased metabolism of *at*RA and 4-oxo-*at*RA is a major contributor to *at*RA resistance. However, it has also been suggested that PXR activation by comedications induces *at*RA clearance in the liver, likely via CYP3A4 induction (Wang et al., 2008). Further in vivo studies involving administration of the metabolites of *at*RA are needed to completely characterize the mechanisms involved in *at*RA resistance and the role that the metabolites may play.

In conclusion, this study shows that CYP26A1 functions primarily as an enzyme that metabolizes *at*RA, 4-OH-*at*RA, 18-OH-*at*RA, and 4-oxo-*at*RA into biologically inactive retinoids and does not contribute to the formation of metabolites with distinct retinoid activity. The results demonstrate that 4-oxo-*at*RA, (4S)-OH-*at*RA, (4R)-OH-*at*RA, and 18-OH-*at*RA induce CYP26A1 and therefore also their own formation. This autoinduction may have broader clinical significance as retinoid resistance is commonly believed to be a result of induction of CYP26A1 in target tissues and cells leading to resistance to therapeutic retinoids. The formation of the most potent inducer of RAR target genes, 4-oxo-*at*RA from 4-OH-*at*RA likely depends on an unidentified microsomal alcohol dehydrogenase suggesting that 4-oxo-*at*RA may have a biological role independent of *at*RA. Further evaluation of the in vivo effects of 4-oxo-*at*RA and 4-OH-*at*RA are warranted to determine the full biological significance of these metabolites and the enzymes forming them.

Molecular Pharmacology Fast Forward. Published on December 9, 2014 as DOI: 10.1124/mol.114.096784
This article has not been copyedited and formatted. The final version may differ from this version.

Acknowledgements

The authors wish to thank Ms Faith Stevison for her skillful assistance with LC-MS/MS.

Molecular Pharmacology Fast Forward. Published on December 9, 2014 as DOI: 10.1124/mol.114.096784
This article has not been copyedited and formatted. The final version may differ from this version.

Authorship Contributions

Participated in research design: Topletz, Tripathy, Foti, Nelson, Isoherranen

Conducted experiments: Topletz, Tripathy, Foti

Contributed new reagents or analytical tools: Topletz, Shimshoni, Nelson

Performed data analysis: Topletz, Tripathy, Foti, Isoherranen

Wrote or contributed to the writing of the manuscript: Topletz, Tripathy, Foti, Nelson, Isoherranen

Molecular Pharmacology Fast Forward. Published on December 9, 2014 as DOI: 10.1124/mol.114.096784
This article has not been copyedited and formatted. The final version may differ from this version.

References

Arnold SL, Amory JK, Walsh TJ, and Isoherranen N (2012) A sensitive and specific method for measurement of multiple retinoids in human serum with UHPLC-MS/MS. *J Lipid Res* **53:**587-598.

Baron JM, Heise R, Blaner WS, Neis M, Joussen S, Dreuw A, Marquardt Y, Saurat JH, Merk HF, Bickers DR, and Jugert FK (2005) Retinoic acid and its 4-oxo metabolites are functionally active in human skin cells in vitro. *J Invest Dermatol* **125:**143-153.

Bonet ML, Ribot J, and Palou A (2012) Lipid metabolism in mammalian tissues and its control by retinoic acid. *Biochim Biophys Acta* **1821:**177-189.

Chambon P (1996) A decade of molecular biology of retinoic acid receptors. *Faseb J* **10:**940-954.

Chithalen JV, Luu L, Petkovich M, and Jones G (2002) HPLC-MS/MS analysis of the products generated from all-trans-retinoic acid using recombinant human CYP26A. *J Lipid Res* **43:**1133-1142.

Chung SS and Wolgemuth DJ (2004) Role of retinoid signaling in the regulation of spermatogenesis. *Cytogenet Genome Res* **105:**189-202.

Creech Kraft J, Lofberg B, Chahoud I, Bochert G, and Nau H (1989) Teratogenicity and placental transfer of all-trans-, 13-cis-, 4-oxo-all-trans-, and 4-oxo-13-cis-retinoic acid after administration of a low oral dose during organogenesis in mice. *Toxicol Appl Pharmacol* **100:**162-176.

Duester G (2008) Retinoic acid synthesis and signaling during early organogenesis. *Cell* **134:**921-931.

Gaemers IC, van Pelt AM, van der Saag PT, and de Rooij DG (1996) All-trans-4-oxo-retinoic acid: a potent inducer of in vivo proliferation of growth-arrested A spermatogonia in the vitamin A-deficient mouse testis. *Endocrinology* **137:**479-485.

Gudas LJ (2012) Emerging roles for retinoids in regeneration and differentiation in normal and disease states. *Biochim Biophys Acta* **1821:**213-221.

Gudas LJ and Wagner JA (2011) Retinoids regulate stem cell differentiation. *J Cell Physiol* **226:**322-330.

Herrmann K (1995) Teratogenic effects of retinoic acid and related substances on the early development of the zebrafish (Brachydanio rerio) as assessed by a novel scoring system. *Toxicology in vitro : an international journal published in association with BIBRA* **9:**267-283.

Hogarth CA and Griswold MD (2013) Retinoic acid regulation of male meiosis. *Curr Opin Endocrin Diab Obes* **20:**217-223.

Idres N, Marill J, Flexor MA, and Chabot GG (2002) Activation of retinoic acid receptor-dependent transcription by all-trans-retinoic acid metabolites and isomers. *J Biol Chem* **277:**31491-31498.

Kane MA, Folias AE, Pingitore A, Perri M, Obrochta KM, Krois CR, Cione E, Ryu JY, and Napoli JL (2010) Identification of 9-cis-retinoic acid as a pancreas-specific autacoid that attenuates glucose-stimulated insulin secretion. *Proc Natl Acad Sci U S A* **107:**21884-21889.

Kane MA, Folias AE, Wang C, and Napoli JL (2008) Quantitative profiling of endogenous retinoic acid in vivo and in vitro by tandem mass spectrometry. *Anal Chem* **80:**1702-1708.

Kewn S, Hoggard PG, Sales SD, Johnson MA, and Back DJ (2000) The intracellular activation of lamivudine (3TC) and determination of 2'-deoxycytidine-5'-triphosphate (dCTP) pools in the presence and absence of various drugs in HepG2 cells. *Br J Clin Pharmacol* **50:**597-604.

Loudig O, Maclean GA, Dore NL, Luu L, and Petkovich M (2005) Transcriptional co-operativity between distant retinoic acid response elements in regulation of Cyp26A1 inducibility. *Biochem J* **392:**241-248.

Lutz JD, Dixit V, Yeung CK, Dickmann LJ, Zelter A, Thatcher JE, Nelson WL, and Isoherranen N (2009) Expression and functional characterization of cytochrome P450 26A1, a retinoic acid hydroxylase. *Biochem Pharmacol* **77:**258-268.

Maden M (2007) Retinoic acid in the development, regeneration and maintenance of the nervous system. *Nat Rev Neurosci* **8:**755-765.

McBurney MW (1993) P19 embryonal carcinoma cells. *Int J Devel Biol* **37:**135-140.

Muindi J, Frankel SR, Miller WH, Jr., Jakubowski A, Scheinberg DA, Young CW, Dmitrovsky E, and Warrell RP, Jr. (1992a) Continuous treatment with all-trans retinoic acid causes a progressive reduction in plasma drug concentrations: implications for relapse and retinoid "resistance" in patients with acute promyelocytic leukemia. *Blood* **79:**299-303.

Muindi JR, Frankel SR, Huselton C, DeGrazia F, Garland WA, Young CW, and Warrell RP, Jr. (1992b) Clinical pharmacology of oral all-trans retinoic acid in patients with acute promyelocytic leukemia. *Cancer research* **52:**2138-2142.

Muindi JR, Roth MD, Wise RA, Connett JE, O'Connor GT, Ramsdell JW, Schluger NW, Romkes M, Branch RA, Sciurba FC, and Investigators FS (2008) Pharmacokinetics and

metabolism of all-trans- and 13-cis-retinoic acid in pulmonary emphysema patients. *J Clin Pharmacol* **48:**96-107.

Napoli JL (2012) Physiological insights into all-trans-retinoic acid biosynthesis. *Biochim Biophys Acta* **1821:**152-167.

Niederreither K, Abu-Abed S, Schuhbaur B, Petkovich M, Chambon P, and Dolle P (2002) Genetic evidence that oxidative derivatives of retinoic acid are not involved in retinoid signaling during mouse development. *Nature Genet* **31:**84-88.

Pijnappel WW, Hendriks HF, Folkers GE, van den Brink CE, Dekker EJ, Edelenbosch C, van der Saag PT, and Durston AJ (1993) The retinoid ligand 4-oxo-retinoic acid is a highly active modulator of positional specification. *Nature* **366:**340-344.

Rhinn M and Dolle P (2012) Retinoic acid signalling during development. *Development* **139:**843-858.

Roberts AB, Lamb LC, and Sporn MB (1980) Metabolism of all-trans-retinoic acid in hamster liver microsomes: oxidation of 4-hydroxy- to 4-keto-retinoic acid. *Arch Biochem Biophys* **199:**374-383.

Samokyszyn VM, Gall WE, Zawada G, Freyaldenhoven MA, Chen G, Mackenzie PI, Tephly TR, and Radominska-Pandya A (2000) 4-Hydroxyretinoic acid, a novel substrate for human liver microsomal UDP-glucuronosyltransferase(s) and recombinant UGT2B7. *J Biol Chem* **275:**6908-6914.

Schug TT, Berry DC, Shaw NS, Travis SN, and Noy N (2007) Opposing effects of retinoic acid on cell growth result from alternate activation of two different nuclear receptors. *Cell* **129:**723-733.

Shimshoni JA, Roberts AG, Scian M, Topletz AR, Blankert SA, Halpert JR, Nelson WL, and Isoherranen N (2012) Stereoselective formation and metabolism of 4-hydroxy-retinoic Acid enantiomers by cytochrome p450 enzymes. *J Biol Chem* **287:**42223-42232.

Tay S, Dickmann L, Dixit V, and Isoherranen N (2010) A comparison of the roles of peroxisome proliferator-activated receptor and retinoic acid receptor on CYP26 regulation. *Mol Pharmacol* **77:**218-227.

Thatcher JE, Buttrick B, Shaffer SA, Shimshoni JA, Goodlett DR, Nelson WL, and Isoherranen N (2011) Substrate specificity and ligand interactions of CYP26A1, the human liver retinoic acid hydroxylase. *Mol Pharmacol* **80:**228-239.

Thatcher JE, Zelter A, and Isoherranen N (2010) The relative importance of CYP26A1 in hepatic clearance of all-trans retinoic acid. *Biochem Pharmacol* **80:**903-912.

Topletz AR, Thatcher JE, Zelter A, Lutz JD, Tay S, Nelson WL, and Isoherranen N (2012) Comparison of the function and expression of CYP26A1 and CYP26B1, the two retinoic acid hydroxylases. *Biochem Pharmacol* **83:**149-163.

Wang T, Ma X, Krausz KW, Idle JR, and Gonzalez FJ (2008) Role of pregnane X receptor in control of all-trans retinoic acid (ATRA) metabolism and its potential contribution to ATRA resistance. *J Pharmacol Exp Ther* **324:**674-684.

White JA, Beckett-Jones B, Guo YD, Dilworth FJ, Bonasoro J, Jones G, and Petkovich M (1997) cDNA cloning of human retinoic acid-metabolizing enzyme (hP450RAI) identifies a novel family of cytochromes P450. *J Biol Chem* **272:**18538-18541.

White JA, Ramshaw H, Taimi M, Stangle W, Zhang A, Everingham S, Creighton S, Tam SP, Jones G, and Petkovich M (2000) Identification of the human cytochrome P450,

P450RAI-2, which is predominantly expressed in the adult cerebellum and is responsible for all-trans-retinoic acid metabolism. *Proc Natl Acad Sci U S A* **97:**6403-6408.

Yamamoto Y, Zolfaghari R, and Ross AC (2000) Regulation of CYP26 (cytochrome P450RAI) mRNA expression and retinoic acid metabolism by retinoids and dietary vitamin A in liver of mice and rats. *Faseb J* **14:**2119-2127.

Yu S, Levi L, Siegel R, and Noy N (2012) Retinoic acid induces neurogenesis by activating both retinoic acid receptors (RARs) and peroxisome proliferator-activated receptor beta/delta (PPARbeta/delta). *J Biol Chem* **287:**42195-42205.

Zhang Y, Zolfaghari R, and Ross AC (2010) Multiple retinoic acid response elements cooperate to enhance the inducibility of CYP26A1 gene expression in liver. *Gene* **464:**32-43.

Footnotes

This work was supported in part by grants from National Institutes of Health [Grant R01 GM081569 and R01 GM111772]. Research reported in this publication was supported in part by the National Center for Advancing Translational Sciences of the National Institutes of Health through the Clinical and Translational Science Awards Program (CTSA) under [Grant TL1TR000422]. The content is solely the responsibility of the authors and does not necessarily represent the official views of the National Institutes of Health.

Molecular Pharmacology Fast Forward. Published on December 9, 2014 as DOI: 10.1124/mol.114.096784
This article has not been copyedited and formatted. The final version may differ from this version.

Legends for Figures

Figure 1: Chemical structures of *at*RA, 4-oxo-*at*RA, (4S)-OH-*at*RA, (4R)-OH-*at*RA, and 18-OH-*at*RA and the proposed metabolic pathways for *at*RA and its metabolites. The specific stereochemistry and the localization of the hydroxylations is shown together with the known enzymatic pathways for the metabolism of *at*RA and its metabolites. The quantitative importance of the indicated enzymes is not known.

Figure 2: Induction of CYP26A1, and RARβ in HepG2 cells treated with *at*RA and its metabolites. Panel A shows the fold-induction of CYP26A1 (white bars) and RARβ (black bars) mRNA by *at*RA, 4-oxo-*at*RA, (4R)-OH-*at*RA, (4S)-OH-*at*RA, and 18-OH- *at*RA after a 1 μM treatment for 48 hours in HepG2 cells. The induction of CYP26A1 (B) and RARβ (C) mRNA by *at*RA, 4-oxo-*at*RA, (4R)-OH-*at*RA, (4S)-OH-*at*RA, and 18-OH-*at*RA in HepG2 cells as a function of inducer concentration is shown in panels B and C. Cells were treated for 48 hours at seven concentrations (ranging from 1 nM to 1 μM) of each substrate, changing media after 24 hours. A vehicle control was EtOH-treated cells and GAPDH was used as a housekeeping gene for RT-PCR analysis.

Figure 3: Induction of CYP26A1, RARβ, CRABP-I and CRABP-II in human hepatocytes. The induction of CYP26A1, RARβ, CRABP-I and CRABP-II mRNA following treatment of human hepatocytes for 2 hours with 100 nM, 500 nM and 1000 nM of *at*RA (panel A), 4-oxo-*at*RA (Panel B), and 4-OH-*at*RA (Panel C), is shown in comparison to vehicle treated cells.

Figure 4. Activation of RARα, RARβ and RARγ by *at*RA, 4-OH-*at*RA and 4-oxo-*at*RA. The activation of RARα, RARβ and RARγ was determined using reporter assays at ligand concentrations between 0 and 2000 nM.

Molecular Pharmacology Fast Forward. Published on December 9, 2014 as DOI: 10.1124/mol.114.096784
This article has not been copyedited and formatted. The final version may differ from this version.

Figure 5. Retinoid and their metabolite concentration versus time profiles in HepG2 cells (panels A-E) and in the cell medium (panels F-J) during a 12 hour treatment. Panels A and F show the detected concentrations following treatment with *at*RA, panels B and G show the concentrations of detected retinoids after treatment with 4-oxo-*at*RA, panels C and H show detected retinoids after treatment with (4R)-OH-*at*RA, panels D and I show detected retinoids after treatment with (4S)-OH-*at*RA and panels E and J the detected concentrations of 18-OH-RA after treatment with this retinoid. HepG2 cells were treated with each inducer (1 μM) and aliquots were taken from the media (panels A-E) at 0, 1, 4, 8 and 12 hours. Cells (panels F-J) were collected for analysis at 1, 4, 8, and 12 hours.

Figure 6. Metabolism of the retinoids following *at*RA and metabolite treatment. *at*RA, (4R)-OH-*at*RA, (4S)-OH-*at*RA, 4-oxo-*at*RA and 18-OH-*at*RA concentrations at 0 (white bars), 12 (black bars), 24 (light grey bars), and 48 (dark grey bars) hours after 1 μM treatment with each of the compounds in HepG2 cells. Medium containing the inducer was changed at 24 hours after a 1 mL aliquot was taken for analysis.

Figure 7. Time course of CYP26A1 mRNA induction and activity in the HepG2 cells following *at*RA and metabolite treatments. Panel A shows the time course of CYP26A1, RARβ and CRABP-I mRNA induction in HepG2 cells following treatment with 1 μM *at*RA. Panels (B) and (C) show the time course of *at*RA-d_5 metabolism during induction with *at*RA. The formation of 4-OH-RA-d_4 (B) and 4-oxo-*at*RA-d_3 (C) after one-hour treatments of *at*RA-d_5 (100 nM) at selected time points (ranging from 0.5 to 48 hours) during the 48 hour treatment with *at*RA (1 μM).

Molecular Pharmacology Fast Forward. Published on December 9, 2014 as DOI: 10.1124/mol.114.096784
This article has not been copyedited and formatted. The final version may differ from this version.

Figure 8. Cofactor dependence in the formation of 4-oxo-*at*RA from 4-OH-*at*RA in human liver microsomes. Human liver microsomes were incubated with 500 nM 4-OH-*at*RA with NADPH, NAD^+ or $NADP^+$ as a cofactor and 4-oxo-*at*RA formation measured. In addition, the inhibition of 4-oxo-*at*RA formation from 4-OH-*at*RA in the presence of NADPH by ketoconazole (10 μM) and talarozole (1 μM) was measured.

Figure 9. Metabolism of 4-oxo-*at*RA and 18-OH-*at*RA by CYP26A1. The depletion of 4-oxo-*at*RA (A) and 18-OH-*at*RA (B) as a function of time was measured at six different concentrations of each substrate and the depletion rates were determined (insets in both panels). All depletion experiments were conducted in duplicate. The depletion constants as a function of substrate concentrations were used to determine the K_m and $k_{dep,max}$ of 4-oxo-*at*RA and 18-OH-*at*RA with CYP26A1.

Molecular Pharmacology Fast Forward. Published on December 9, 2014 as DOI: 10.1124/mol.114.096784
This article has not been copyedited and formatted. The final version may differ from this version.

Tables

Table 1. Effect of *at*RA, 4-OH-*at*RA and 4-oxo-*at*RA on RARα, RARβ and RARγ activation in reporter assays.

Treatment	EC_{50} nM (95% confidence interval)		
	RARα	RARβ	RARγ
***at*RA**	**19 (13-30)**	**1 (0.7-1.5)**	**4 (3-6)**
4-OH-*at*RA	**114 (91-141)**	**53 (33-84)**	**45 (37-54)**
4-oxo-*at*RA	**61 (47-80)**	**9 (5-14)**	**15 (11-20)**

Molecular Pharmacology Fast Forward. Published on December 9, 2014 as DOI: 10.1124/mol.114.096784
This article has not been copyedited and formatted. The final version may differ from this version.

Table 2. The 0-12 hour exposures (AUCs) of each retinoid and its metabolites in in HepG2 cells and in media, cell-to-medium ratios, and the observed CYP26A1 mRNA induction after a 1 μM treatment of the cells with the test compound.

Treatment	Inducer AUC^{0-12hr} in Cells (nmoles•hour/mL)	Metabolite AUC^{0-12hr} in Cells (nmoles•hour/mL)	Inducer AUC^{0-12hr} in Medium (nmoles•hour/mL)	Metabolite AUC^{0-12hr} in Medium (nmoles•hour/mL)
*at*RA	3750 ± 350	130 ± 6 (4-oxo-*at*RA) 120 ± 2 (4-OH-*at*RA)	10.3 ± 1.0	BLQ* (4-oxo-*at*RA) BLQ* (4-OH-*at*RA)
4-oxo-*at*RA	980 ± 40	270 ± 10 (4-OH-*at*RA)	7.9 ± 0.9	2.4 ± 0.2 (4-OH-*at*RA)
(4R)-OH-*at*RA	570 ± 90	340 ± 30 (4-oxo-*at*RA)	5.4 ± 0.1	1.0 ± 0.1 (4-oxo-*at*RA)
(4S)-OH-*at*RA	300 ± 10	630 ± 7 (4-oxo-*at*RA)	4.3 ± 0.1	4.1 ± 0.2 (4-oxo-*at*RA)
18-OH-*at*RA	1740 ± 70	------	12.3 ± 0.1	------

Treatment	Inducer Cell-to-Medium AUC^{0-12hr} Ratio	Metabolite Cell-to-Medium AUC^{0-12hr} Ratio	CYP26A1 mRNA (fold increase)
*at*RA	363 (*at*RA)	n/a (4-oxo-*at*RA) n/a (4-OH-*at*RA)	3700 ± 180
4-oxo-*at*RA	123	112 (4-OH-*at*RA)	2980 ± 250
(4R)-OH-*at*RA	106	354 (4-oxo-*at*RA)	1350 ± 230
(4S)-OH-*at*RA	70	155 (4-oxo-*at*RA)	1360 ± 240
18-OH-*at*RA	141	------	300 ± 90

*BLQ: Below the limit of quantification

Molecular Pharmacology Fast Forward. Published on December 9, 2014 as DOI: 10.1124/mol.114.096784
This article has not been copyedited and formatted. The final version may differ from this version.

Table 3. The 0-2 hour exposures (AUCs) of each retinoid and its metabolites in human primary hepatocytes.

Treatment	**Inducer AUC^{0-2hr} in medium (nmoles/hour•ml)**	**Metabolites AUC^{0-2hr} in medium (nmoles/hour•ml)**
*at*RA (100nM)	302 ± 7	BLQ
*at*RA (500nM)	1305 ± 16	BLQ
*at*RA (1μM)	2810 ± 62	0.6 ± 0.4 (4-oxo-*at*RA)
4-OH-*at*RA (100nM)	277 ± 5	11 ± 2 (4-oxo-*at*RA)
4-OH-*at*RA (500nM)	848 ± 6	90 ± 5 (4-oxo-*at*RA)
4-OH-*at*RA (1μM)	2018 ± 12	309 ± 20 (4-oxo-*at*RA)
4-oxo-*at*RA (100nM)	172 ± 3	0 (4-OH-*at*RA)
4-oxo-*at*RA (500nM)	728 ± 10	6.5 ± 0.5 (4-OH-*at*RA)
4-oxo-*at*RA (1μM)	1584 ± 29	11 ± 2 (4-OH-*at*RA)

*BLQ: Below the limit of quantification

Molecular Pharmacology Fast Forward. Published on December 9, 2014 as DOI: 10.1124/mol.114.096784
This article has not been copyedited and formatted. The final version may differ from this version.

Table 4. The effect of selective P450 and alcohol dehydrogenase inhibitors on 4-oxo-*at*RA or 4-OH-*at*RA formation from *at*RA and formation of 4-OH-*at*RA from 4-oxo-*at*RA in HepG2 cells. The inhibitors used were 4-methylpyrazole (250 μM, alcohol dehydrogenases), cimetidine (250 μM, alcohol dehydrogenases), ketoconazole (10μM, P450s), talarozole (1μM, CYP26), testosterone (25 μM, aldo-keto reductases), or carbenoxolone (25 μM and 50μM, retinol dehydrogenases). Significant changes in comparison to no inhibitor controls were performed using the Student's unpaired t-test and are indicated as $*P < 0.05$.

Treatment	**4-oxo-*at*RA Formation (% of Control)**	**4-OH-*at*RA Formation (% of Control)**
*at*RA (control)	100 ± 3	100 ± 7
*at*RA + 4-methylpyrazole	109 ± 8	122 ± 11
*at*RA+cimetidine	130 ± 6*	149 ± 5*
*at*RA+ketoconazole (10μM)	20 ± 1*	16 ± 6*
*at*RA+testosterone	109 ± 6	133 ± 4*
*at*RA + carbenoxolone (25 μM)	74 ± 3*	92 ± 22
*at*RA + carbenoxolone (50 μM)	80 ± 8*	99 ± 25
*at*RA + talarozole (1μM)	20 ± 3*	0
Treatment	**4-oxo-RA Formation (% of Control)**	**4-OH-RA Depletion (% of Control)**
4-OH-*at*RA (Control)	100 ± 6	100 ± 6
4-OH-*at*RA + 4-methylpyrazole	121 ± 12	96 ± 3
4-OH-*at*RA + cimetidine	121 ± 3*	99 ± 2
4-OH-*at*RA + ketoconazole	110 ± 0	75 ± 0*
4-OH-*at*RA + testosterone	107 ± 1	107 ± 0
4-OH-*at*RA + carbenoxolone (25 μM)	115 ± 9	80 ± 9*
4-OH-*at*RA + carbenoxolone (50 μM)	117 ± 6*	96 ± 3

Molecular Pharmacology Fast Forward. Published on December 9, 2014 as DOI: 10.1124/mol.114.096784
This article has not been copyedited and formatted. The final version may differ from this version.

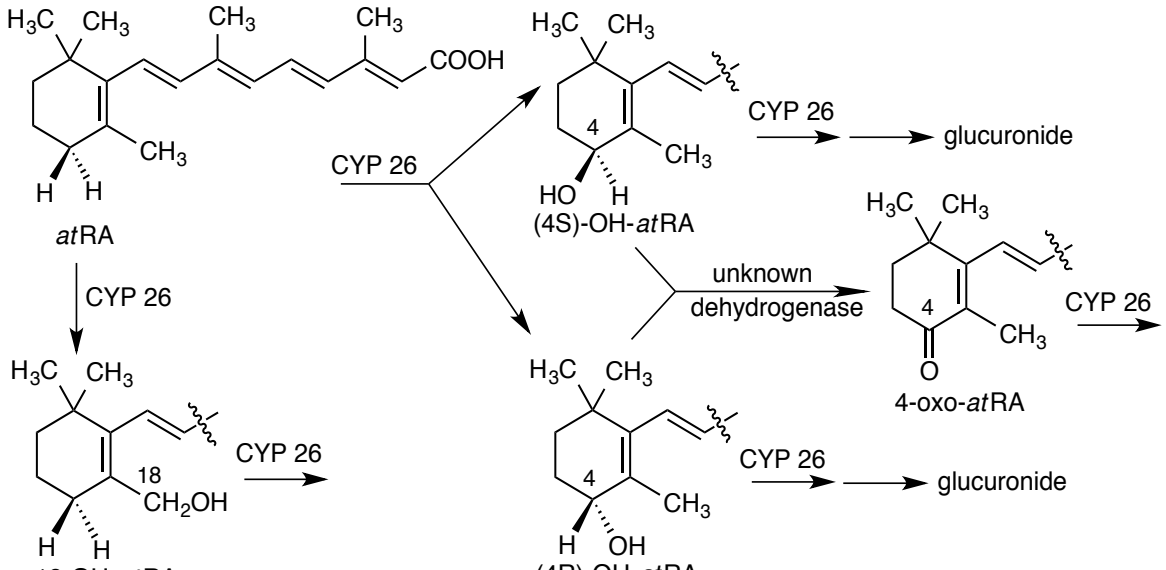

Figure 1

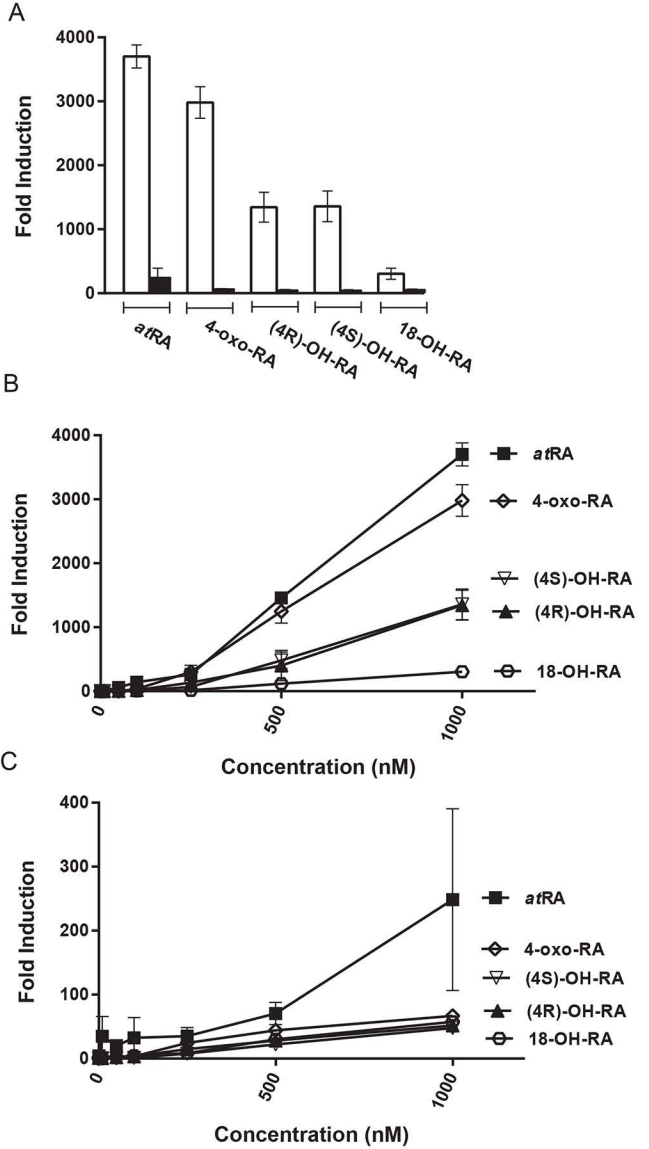
A
Fold Induction
4000
3000
2000
1000
0
atRA
4-oxo-RA
(4R)-OH-RA
(4S)-OH-RA
18-OH-RA
B
Fold Induction
4000
3000
2000
1000
0
atRA
4-oxo-RA
(4S)-OH-RA
(4R)-OH-RA
18-OH-RA
0
500
1000
Concentration (nM)
C
Fold Induction
400
300
200
100
0
atRA
4-oxo-RA
(4S)-OH-RA
(4R)-OH-RA
18-OH-RA
0
500
1000
Concentration (nM)

Figure 2

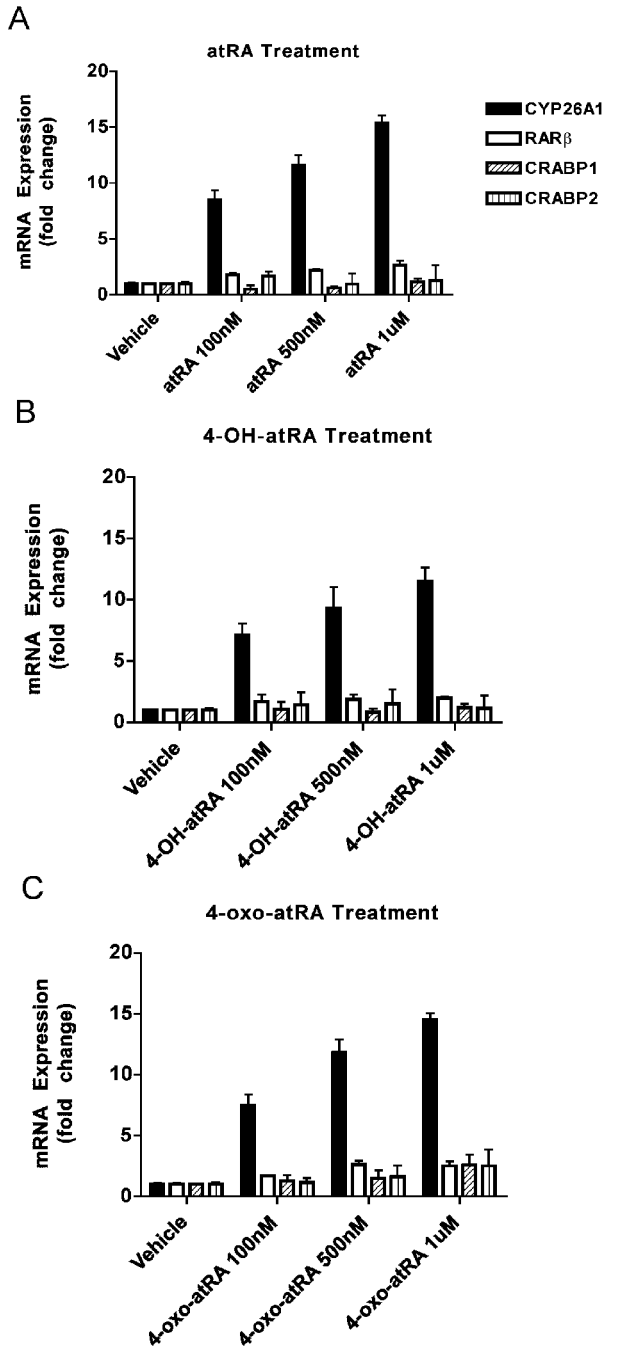
A
atRA Treatment
mRNA Expression (fold change)
20
15
10
5
0
CYP26A1
RARβ
CRABP1
CRABP2
Vehicle
atRA 100nM
atRA 500nM
atRA 1uM
B
4-OH-atRA Treatment
mRNA Expression (fold change)
20
15
10
5
0
Vehicle
4-OH-atRA 100nM
4-OH-atRA 500nM
4-OH-atRA 1uM
C
4-oxo-atRA Treatment
mRNA Expression (fold change)
20
15
10
5
0
Vehicle
4-oxo-atRA 100nM
4-oxo-atRA 500nM
4-oxo-atRA 1uM

Figure 3

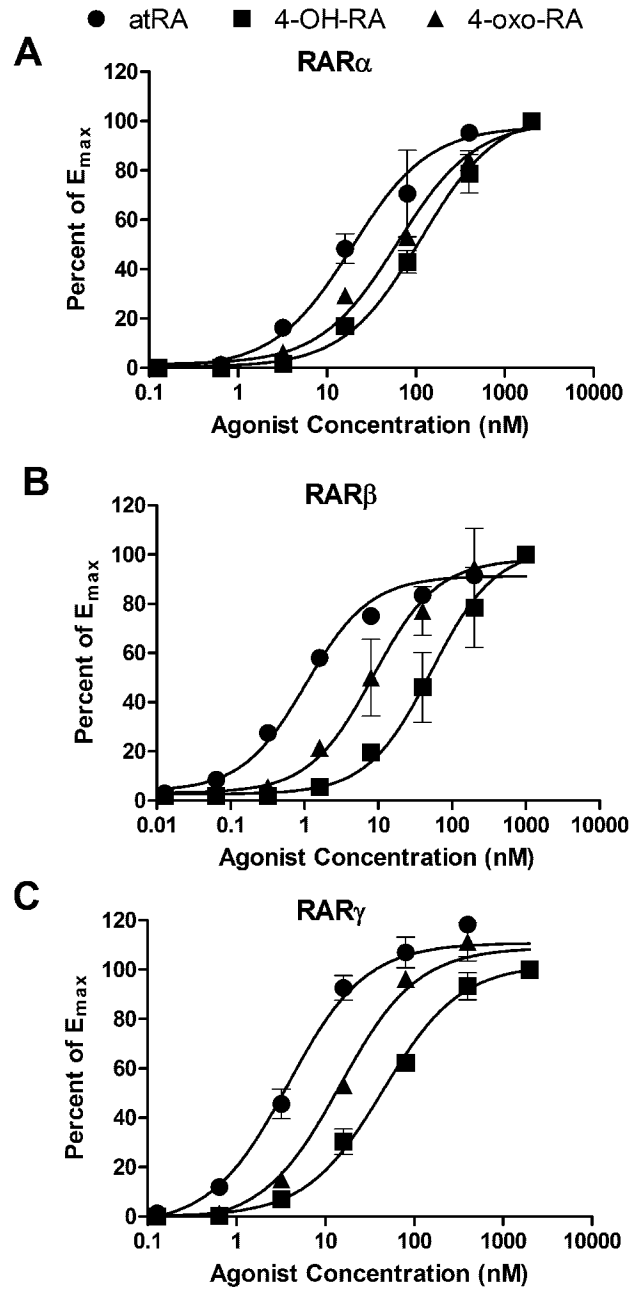
atRA
4-OH-RA
4-oxo-RA
A
RARα
Percent of Emax
120
100
80
60
40
20
0
0.1
1
10
100
1000
10000
Agonist Concentration (nM)
B
RARβ
Percent of Emax
120
100
80
60
40
20
0
0.01
0.1
1
10
100
1000
10000
Agonist Concentration (nM)
C
RARγ
Percent of Emax
120
100
80
60
40
20
0
0.1
1
10
100
1000
10000
Agonist Concentration (nM)

Figure 4

Molecular Pharmacology Fast Forward. Published on December 9, 2014 as DOI: 10.1124/mol.114.096784
This article has not been copyedited and formatted. The final version may differ from this version.

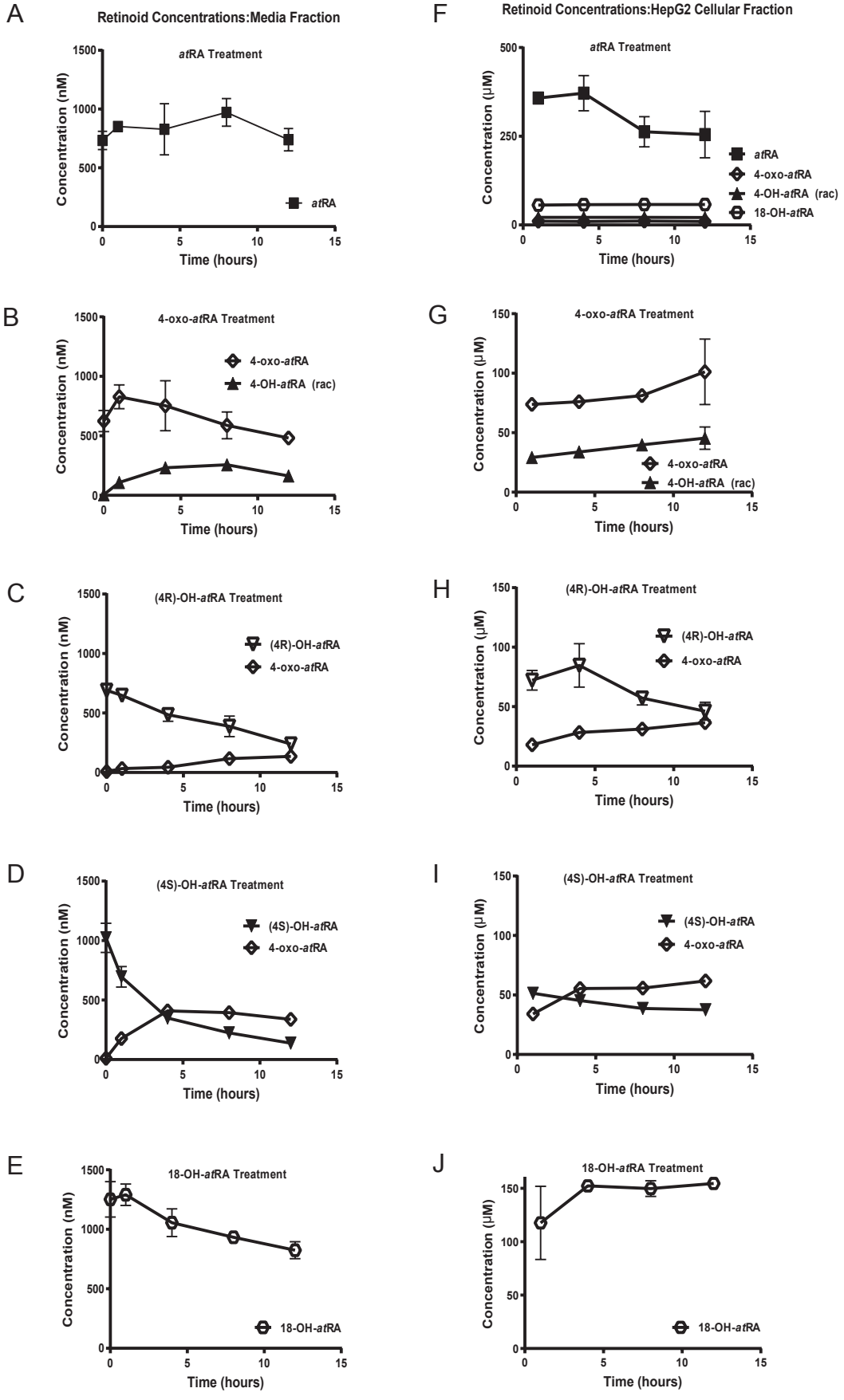

Figure 5

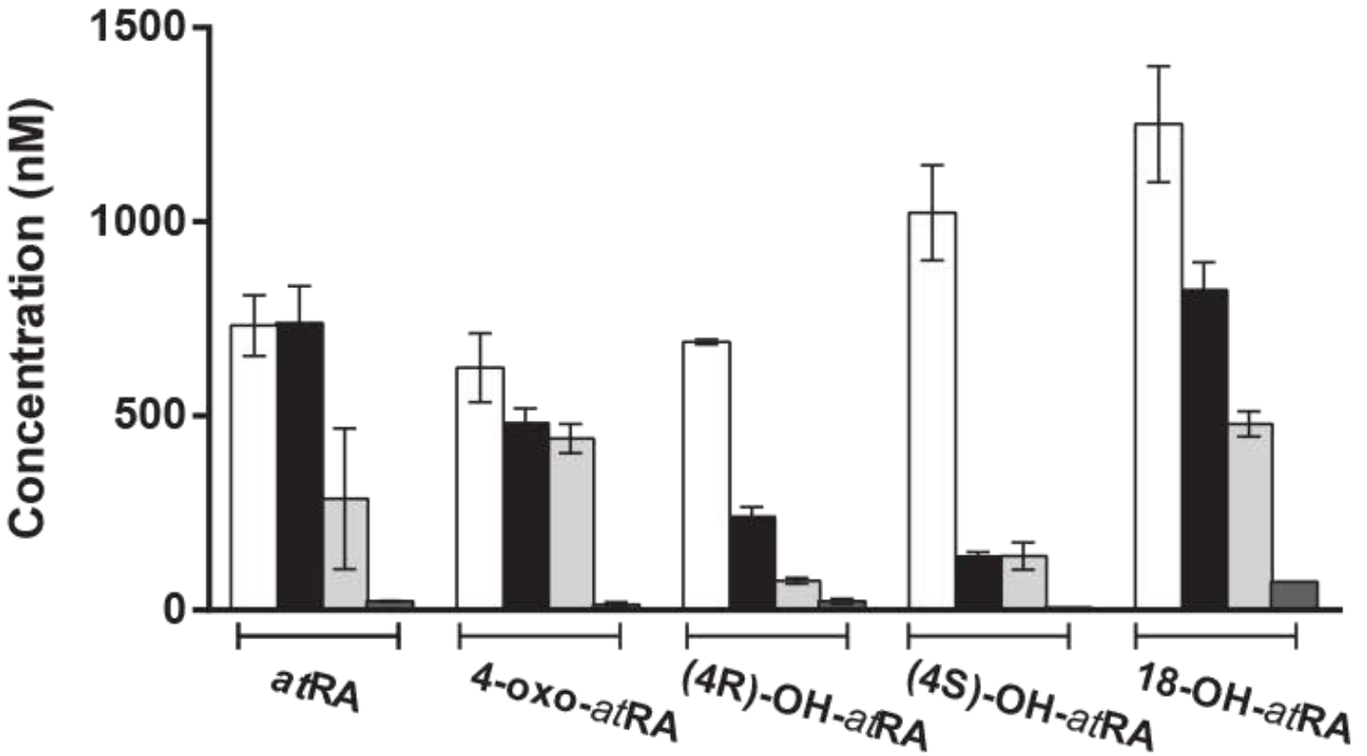
Concentration (nM)
1500
1000
500
0
atRA
4-oxo-atRA
(4R)-OH-atRA
(4S)-OH-atRA
18-OH-atRA

Figure 6

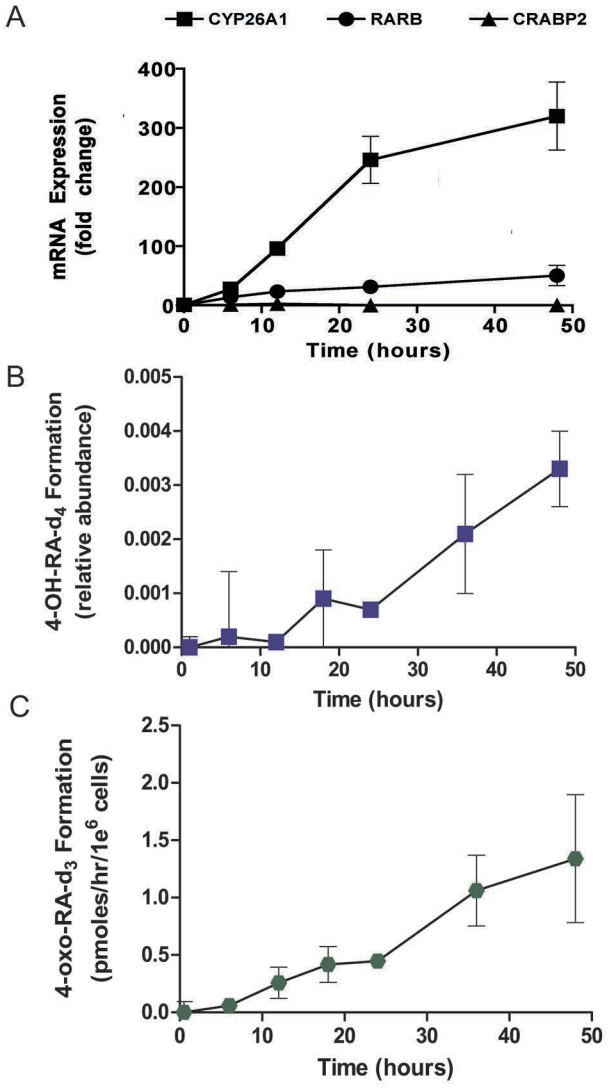
A
CYP26A1
RARB
CRABP2
mRNA Expression (fold change)
400
300
200
100
0
0
10
20
30
40
50
Time (hours)
B
4-OH-RA-d4 Formation (relative abundance)
0.005
0.004
0.003
0.002
0.001
0.000
0
10
20
30
40
50
Time (hours)
C
4-oxo-RA-d3 Formation (pmoles/hr/1e6 cells)
2.5
2.0
1.5
1.0
0.5
0.0
0
10
20
30
40
50
Time (hours)

Figure 7

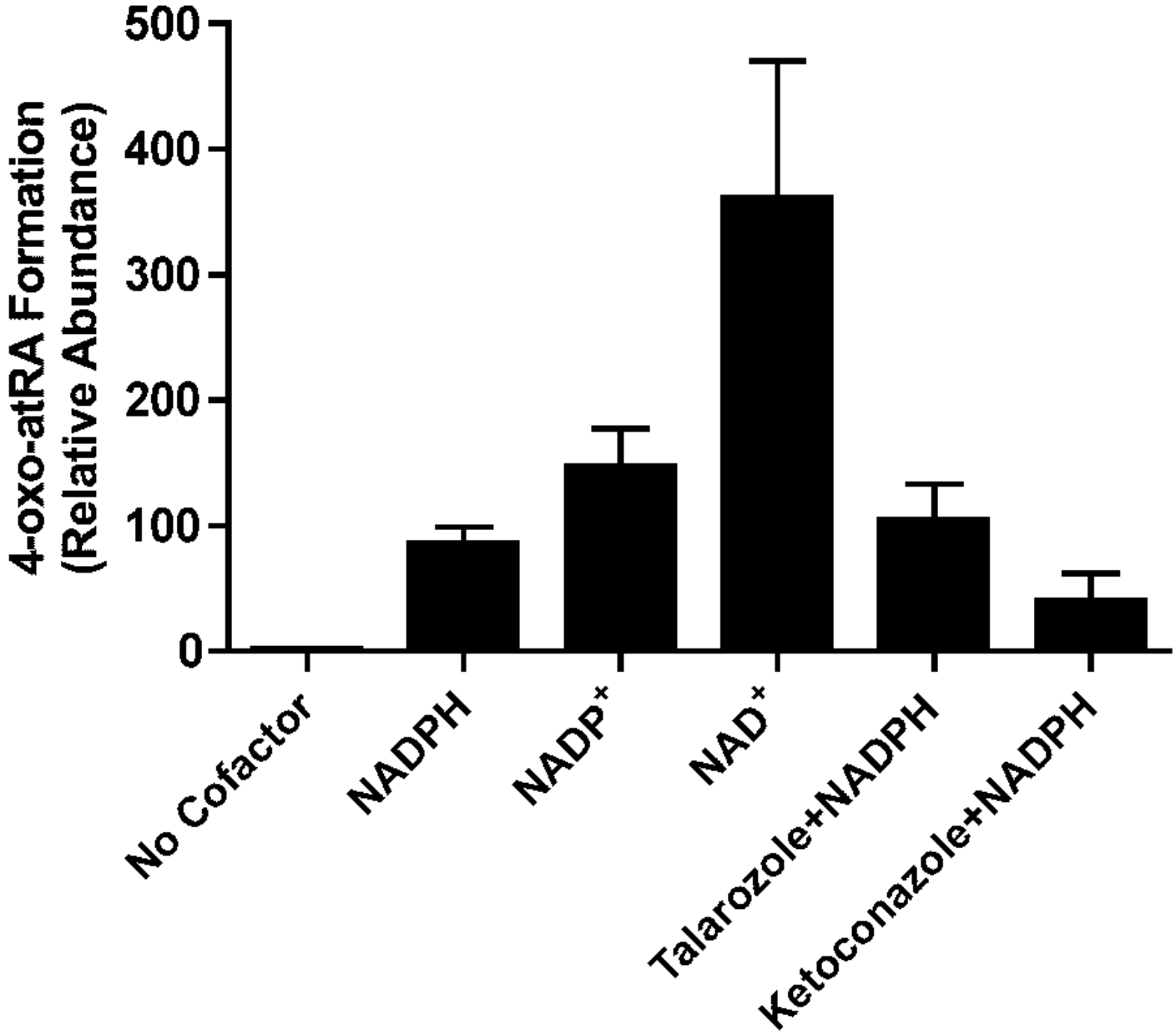
4-oxo-atRA Formation
(Relative Abundance)
500
400
300
200
100
0
No Cofactor
NADPH
NADP+
NAD+
Talarozole+NADPH
Ketoconazole+NADPH

Figure 8

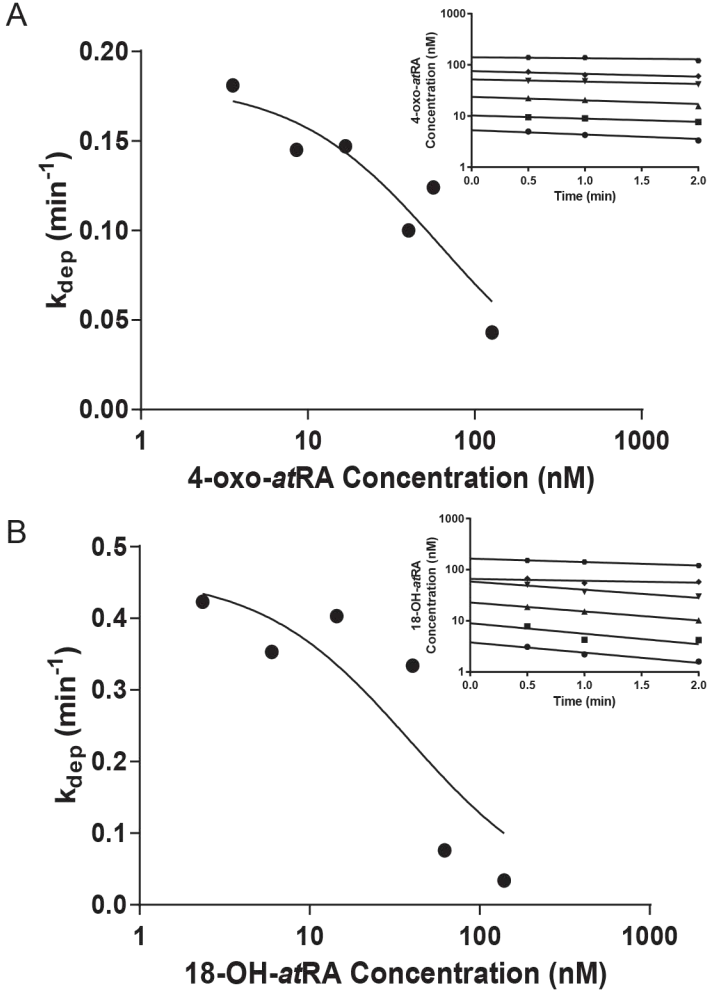
A
0.20
0.15
0.10
0.05
0.00
k_{dep} (min^{-1})
1
10
100
1000
4-oxo-*at*RA Concentration (nM)
4-oxo-*at*RA Concentration (nM)
1000
100
10
1
0.0
0.5
1.0
1.5
2.0
Time (min)
B
0.5
0.4
0.3
0.2
0.1
0.0
k_{dep} (min^{-1})
1
10
100
1000
18-OH-*at*RA Concentration (nM)
18-OH-*at*RA Concentration (nM)
1000
100
10
1
0.0
0.5
1.0
1.5
2.0
Time (min)

Figure9